Vibron solitons

Xidi Wang
Department of Physics (B-019), University of California, San Diego, La Jolla, California 92093

David W. Brown
Institute for Nonlinear Science (R-002), University of California, San Diego, La Jolla, California 92093

Katja Lindenberg
Department of Chemistry (B-040) and Institute for Nonlinear Science (R-002), University of California, San Diego, California 92093

(Received 19 September 1988)

Starting from a general Hamiltonian describing the dynamics of vibrons coupled to acoustic phonons, equations of motion for the dynamical variables are obtained by eliminating the phonon degrees of freedom. Specific results are obtained for the form of this Hamiltonian proposed by Takeno. Vibron number is not conserved in general, which distinguishes our study from others based on the Fröhlich Hamiltonian in which the analogous bosons are conserved. Solitary-wave solutions are found for approximate continuum wave equations obtained employing a coherent-state ansatz under a rotating-wave approximation. Regimes of validity are determined, and within these regimes physically meaningful quantities are computed, including energy–wave-vector relations, frequency–wave-vector relations, binding energies, and effective masses. The role of these in spectroscopy is discussed. Several instabilities are encountered and their origins traced. Certain of these are argued to be generic and intrinsic to the physics of the problem, while others can be shown to be artifacts of the particular model chosen for specific calculations. The modification of our results caused by discreteness corrections is considered, and the role of thermal fluctuations is discussed.

I. INTRODUCTION

Making progress in understanding the role of soliton dynamics in physical systems is hampered by the enormous difficulty in treating any nonlinear evolution other than one of the few well-known integrable families such as the nonlinear Schrödinger family. The great potential for soliton dynamics is that despite the complex and multifarious textures presented to us by nature, the universality of the nonlinear Schrödinger and other soliton familes causes them to be implicit under the surface of many physical transport problems. This great potential is simultaneously a great problem, since universal qualities tell us little about the properties of particular systems or situations, and belief in universality can lead us to imbue physical systems with properties they may not have. It is in this light that we approach a problem of widespread current interest from a perspective somewhat separated from the conventional point of view.

Envelope solitons in one-dimensional molecular systems have been studied intensively since first proposed by Davydov and Kislukha.[1] One can fairly say that there is not one theory of molecular solitons, but many. Davydov's original theory,[1] which first recognized the possibility of nondispersive propagation, continued the development contributed to by numerous workers[2–8] from Landau[2] to Holstein.[7] More recent generalizations can be distinguished by the manner and extent to which the quantum character of the bare particle is taken into account. Most deal with one of two ansatz states proposed by Davydov[9,10] and apply Hamilton's equations,[11–18] semiclassical quantization procedures,[19,20] Heisenberg equations,[21–24] Schrödinger equations,[25–29] Liouville–von Neumann equations,[30] or derive alternative equations of motion by variational methods.[31–33]

Davydov's original theory was developed for application to systems at zero temperature. More recently, great interest in the possible role of solitons in biological settings has raised important questions about the stability of solitons at elevated (e.g., physiological) temperatures. Little progress on the finite-temperature problem has been made by analytic theory. Numerical simulations of an α-helix model by Lomdahl and Kerr[15] and by Lawrence *et al.*[16] suggest that solitons are unstable in that system at room temperature. Other simulations based on a different model have been interpreted as indicating room-temperature stability.[17]

On the other hand, Takeno[34–36] has observed that as a model of the amide-I vibration in the α helix, Davydov's approach fails to include some of the basic properties which distinguish vibrons from conserved particles. Takeno proposed an improved model and showed that while many similarities exist between its consequences and those which follow from the Davydov model, significant differences could be found, including larger binding energies suggestive of greater stability. Takeno's improved model has been applied to the α helix in numerical simulations by Lomdahl and Kerr,[37] with results indicating stability greater than that of the corresponding Davydov model. The relationshp between the Davydov model and

Takeno's improved model can be understood as follows.

We start with a general system Hamiltonian having the following form:

$$\hat{H}=\hat{H}_{\rm sys}+\hat{H}_{\rm ph}+\hat{H}_{\rm int}\ , \tag{1.1a}$$

where $\hat{H}_{\rm sys}$ is the Hamiltonian of the system of interest, expressed as a function of a set of position and momentum operators $\{\hat{q},\hat{p}\}$. (We find it convenient to use the position-momentum representation for the system variables rather than the second-quantized formalism.) $\hat{H}_{\rm ph}$ is the phonon and/or bath Hamiltonian which may generally contain any type phonon modes and any number of branches; however, we take $\hat{H}_{\rm ph}$ to be strictly harmonic. $\hat{H}_{\rm int}$ is an interaction Hamiltonian which is linear in the position coordinates of the molecules comprising the lattice.

$$\hat{H}_{\rm sys}=H_{\rm sys}\{\hat{q},\hat{p}\}\ , \tag{1.1b}$$

$$\hat{H}_{\rm ph}=H_{\rm ph}\{\hat{Q},\hat{P}\}\ , \tag{1.1c}$$

$$\hat{H}_{\rm int}=\sum_m \hat{Q}_m g_m\{\hat{q},\hat{p}\}\ . \tag{1.1d}$$

$g_m\{\hat{q},\hat{p}\}$ is the force experienced by the molecule m at its equilibrium position R_m due to the presence and dynamics of the system excitations. The only formal constraint on $g_m\{\hat{q},\hat{p}\}$ is that it be Hermitian; however, in specific calculations below we will be concerned with models for which the relevant phonons are of the longitudinal acoustic modes, and the influence of a localized excitation on neighboring molecules is symmetric and extends only to nearest neighbors; that is,

$$g_m\{\hat{q},\hat{p}\}=g(\hat{q}_{m-1})-g(\hat{q}_{m+1})\ . \tag{1.2}$$

We then arrive at the Hamiltonian proposed by Takeno for the description of vibron transport

$$\hat{H}_{\rm Takeno}=\hat{H}_{\rm vib}+\hat{H}_{\rm ph}+\hat{H}_{\rm vib\text{-}ph}\ , \tag{1.3a}$$

where

$$\hat{H}_{\rm vib}=\sum_n\left[\frac{\hat{p}_n^{\,2}}{2m}+v(\hat{q}_n)\right]-\sum_{m,n}L_{mn}\hat{q}_m\hat{q}_n\ , \tag{1.3b}$$

$$\hat{H}_{\rm ph}=\sum_n\left[\frac{\hat{P}_n^{\,2}}{2M}+\frac{w}{2}(\hat{Q}_n-\hat{Q}_{n-1})^2\right]\ , \tag{1.3c}$$

$$\hat{H}_{\rm vib\text{-}ph}=\sum_n(\hat{Q}_{n+1}-\hat{Q}_{n-1})g(\hat{q}_n)\ . \tag{1.3d}$$

$\hat{H}_{\rm vib}$ is the Hamiltonian of a set of oscillators having local potentials $v(\hat{q}_n)$. L_{mn} is the transfer coefficient arising from the coupling of the mth and nth intracell oscillations. Such coupling may arise from electronic dipoles, as is apparently the case in acetanilide[14] and α-helix proteins,[38] or may be purely mechanical in origin, as is apparently the case in L-alanine.[39] We assume $L_{mn}=L_{nm}$. $\hat{q}_n$ is the displacement operator of the oscillator in the nth molecular unit, $\hat{p}_n$ is the conjugate momentum operator, and m is the appropriate reduced mass. $\hat{Q}_n$ and $\hat{P}_n$ are the displacement and momentum operators of the nth molecular unit which has mass M, and w is the longitudinal stiffness coefficient. The interaction between the local modes and acoustic phonons is given by the interaction Hamiltonian $\hat{H}_{\rm vib\text{-}ph}$. In general, both the potentials $v(\hat{q}_n)$ and the forces $g(\hat{q}_n)$ may be arbitrary functions of $\hat{q}_n$; however, we consider the leading order in $\hat{q}_n$ to be quadratic, such that

$$v(\hat{q}_n)=\tfrac{1}{2}m\omega_v^2\hat{q}_n^{\,2}+\cdots,\quad g(\hat{q}_n)=g\hat{q}_n^{\,2}+\cdots\ . \tag{1.4}$$

A useful special case of the general Takeno model retains only the leading orders in the above series. We call this specialized Hamiltonian the *quadratic Takeno Hamiltonian,* since both $v(q_n)$ and $g(q_n)$ are quadratic functions of q_n.

Also contained in the general Hamiltonian (1.1) is the Fröhlich Hamiltonian,[5] a special case of which is the basis of the Davydov model

$$\hat{H}_{\rm Davydov}=\hat{H}_{\rm ex}+\hat{H}_{\rm ph}+\hat{H}_{\rm ex\text{-}ph}\ , \tag{1.5a}$$

where

$$\hat{H}_{\rm ex}=\sum_n Ea_n^\dagger a_n-\sum_{m,n}J_{mn}a_m^\dagger a_n\ , \tag{1.5b}$$

$$\hat{H}_{\rm ph}=\sum_n\left[\frac{\hat{P}_n^{\,2}}{2M}+\frac{w}{2}(\hat{Q}_n-\hat{Q}_{n-1})^2\right]\ , \tag{1.5c}$$

$$\hat{H}_{\rm ex\text{-}ph}=\sum_n\chi(\hat{Q}_{n+1}-\hat{Q}_{n-1})a_n^\dagger a_n\ . \tag{1.5d}$$

$\hat{H}_{\rm Davydov}$ can be viewed as a number-conserving truncation of the quadratic Takeno Hamiltonian; indeed, the expectation values of $\hat{H}_{\rm Takeno}$ (quadratic) and $\hat{H}_{\rm Davydov}$ in any state containing a definite number of a-bosons are identical provided the a-bosons are those associated with the decoupled local oscillators:

$$\hat{q}_n=\left[\frac{\hbar}{2m\omega_v}\right]^{1/2}(a_n^\dagger+a_n)\ , \tag{1.6a}$$

$$\hat{p}_n=i\left[\frac{m\hbar\omega_v}{2}\right]^{1/2}(a_n^\dagger-a_n)\ , \tag{1.6b}$$

and one makes the proper identifications of the various Hamiltonian parameters

$$J_{mn}=\frac{\hbar L_{mn}}{m\omega_v},\quad E=\hbar\omega_v,\quad \chi=\frac{\hbar g}{m\omega_v}\ . \tag{1.6c}$$

[The reader is reminded that the relations (1.6a) and (1.6b) are defining relations for a_n and $a_n^\dagger$, not $\hat{q}_n$ and $\hat{p}_n$.] Since the potential $v(\hat{q}_n)$ may be anharmonic, the creation and annihilation operators $a_n^\dagger$ and a_n defined by the harmonic oscillator relations (1.6a) and (1.6b) do not diagonalize intracell oscillations in the general case.

It is straightforward to show that in both the Davydov and Takeno models the dynamics of free excitations can be characterized in part by maximum speeds $v_{\rm max}^D$, and $v_{\rm max}^D$, respectively; however in the continuum limit one finds that

$$v^D_{\max}\to\infty, \quad v^T_{\max}\to v_f\equiv\left[\frac{2Ll^2}{m}\right]^{1/2}, \tag{1.7a}$$

$$E^D(k)\to E^D(0)+\frac{\hbar^2k^2}{2m^D}, \quad \omega(k)\to[\omega^2(0)+k^2v_f^2]^{1/2}, \tag{1.7b}$$

$$m^D=\frac{\hbar^2}{2Jl^2}, \quad m^T=\frac{\hbar\omega(0)}{v_f^2}. \tag{1.7c}$$

(See Fig. 1.) A wave vector k_0 can be defined through the relation $\hbar k_0=m^Tv_f$ which sets the scale for structure in **k** space. No corresponding quantity exists in the continuum limit of the Davydov model.

In the continuum limit, the linear-wave equation implicit in the Davydov model is the Schrödinmger equation, while that underlying the Takeno model is the Klein-Gordon equation. One consequence of this fact is that continuum treatments of the Davydov model implicitly presume material properties consistent with the speed of sound v_a being small relative to the maximum group velocity attainable by a free excitation, $v^D_{\max}$. On the other hand, (1.7a) shows that while the Takeno model subsumes such cases, it also allows one to consider materials for which $v_f<v_a$. The relation $v_f<v_a$ is typical of "narrow-band" systems, while $v_f>v_a$ is typical of "wide-band" systems. We will consider both types of systems below.

In this paper we present an analysis of the Takeno model using the methods of Brown *et al.*[30] and Wang *et al.*[18] This analysis parallels that given for the Davydov model in Ref. 18. As in Ref. 18, effects appear which are not found in previous analyses of the model. In Sec. II we present the exact dynamics of the quadratic Takeno model in the Heisenberg representation. In Sec. III we discuss the use of coherent states and obtain the approximate equations of motion upon which further analysis is based. In Sec. IV we obtain approximate solitary-wave solutions in the continuum limit. The total energy, binding energy, carrier wave frequency, effective mass, and the length scale of the carrier wave modulation (width of the solitary wave) are determined. Regimes of validity are mapped out and the role of the acoustic sound speed is examined. In Sec. V the various instabilities we encounter are laid out and the significance of each is assessed. In Sec. VI we reexamine the equations of motion of Sec. III with the aim of assessing the impact of the discreteness of real lattices on the character of solitary-wave states. In Sec. VII we indicate how our approximation may be applied to obtain corresponding results for the general Takeno model. In Sec. VIII we discuss thermal effects by comparing the character of thermal fluctuations in the Davydov and Takeno models. A qualitative description of thermalization is given in which a unique minimum-energy envelope plays the central role. Our conclusions are summarized in Sec. IX.

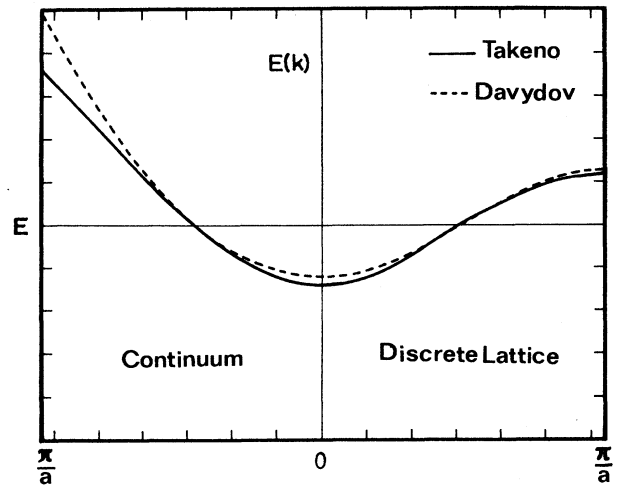

FIG. 1. Linear dispersion relations for the Takeno model (——) and the Davydov model (— — —). The right-hand panel shows dispersion relations for a discrete lattice having a lattice constant a, while the left-hand panel shows corresponding dispersion relations for a continuous medium. Note that under this mapping the band edges and effective masses of the linear excitations are different in the two models and that the distinction is preserved in the continuum limit.

II. DYNAMICS IN THE HEISENBERG PICTURE

We now obtain exact Heisenberg equations of motion for the vibron subsystem by eliminating acoustic phonon variables. For this purpose it is convenient to represent the lattice degrees of freedom using the second-quantized operators b_q and $b_q^\dagger$ defined by the relations

$$\hat{Q}_n=\sum_q\left[\frac{\hbar}{2NM\omega_q}\right]^{1/2}e^{-iqR_n}(b_q^\dagger+b_{-q}), \tag{2.1a}$$

$$\hat{P}_n=\sum_q i\left[\frac{M\hbar\omega_q}{2N}\right]^{1/2}e^{-iqR_n}(b_q^\dagger-b_{-q}), \tag{2.1b}$$

where ω_q is the phonon dispersion relation, which for longitudinal acoustic phonons is

$$\omega_q=\omega_B\sin(|ql|/2). \tag{2.2}$$

For simplicity, we limit our present discussion to the quadratic Takeno model [cf. (1.4)] for which the Heisenberg equations of motion for the elementary vibron and phonon operators are

$$\dot{\hat{q}}_n=\frac{\hat{p}_n}{m}, \tag{2.3a}$$

$$\dot{\hat{p}}_n=-m\omega_v^2\hat{q}_n+2\sum_m L_{mn}\hat{q}_m-2\sum_q g_n^q\hbar\omega_q(b_q^\dagger+b_{-q})q_n, \tag{2.3b}$$

$$\dot{b}_q=-i\omega_qb_q-i\sum_{q,m}g_m^q\omega_q\hat{q}^2_m, \tag{2.3c}$$

where

$$g_m^q=\frac{g[-2i\sin(ql)]}{(2NM\hbar\omega_q^3)^{1/2}}e^{-iqR_m}. \tag{2.4}$$

Integrating the equation for the phonon variables (2.3c), we obtain the exact relation

$$b_q(t)=e^{-i\omega_q t}b_q(0) -i\int_0^t d\tau\, e^{-i\omega_q(t-\tau)}\sum_m g_m^q\omega_q\hat{q}_m^2(\tau)\ . \tag{2.5}$$

The first term propagates according to the free evolution of the phonon system, and the second accounts for the disturbance of the free-phonon evolution by the vibron system.

Although $b_q(t)$ and $\hat{q}_n(t')$ commute at equal times ($t=t'$), they do not commute at different times ($t\neq t'$). One consequence of this is that the terms on the rhs of (2.5) do not commute with each other, nor do they commute with other operators appearing in the equations of motion. When substituting (2.5) into (2.3b), therefore, we are free to make the ordering of our choice as long as the same ordering is chosen for both contributions to (2.5). For the (quadratic) Takeno Hamiltonian (1.3) we find the operator equations

$$\dot{\hat{q}}_n(t)=\frac{\hat{p}_n(t)}{m}\ , \tag{2.6a}$$

$$\dot{\hat{p}}_n(t)=-m\omega_v^2\hat{q}_n(t)+2\sum_m L_{mn}\hat{q}_m(t)-2\hat{F}_n(t)\hat{q}_n(t) -2\sum_l\int_0^t d\tau\,\dot{K}_{nl}(t-\tau)\hat{q}_l^2(\tau)\hat{q}_n(t)\ . \tag{2.6b}$$

The integral kernels are given by

$$K_{mn}(t)\equiv 2\sum_q g_m^q g_n^{-q}\hbar\omega_q\cos(\omega_q t)\ , \tag{2.7}$$

and the fluctuation operators $\hat{F}_n(t)$ are proportional to those appearing in Refs. 18, 21, and 30

$$\hat{F}_n(t)\equiv\sum_q g_m^q\hbar\omega_q[e^{i\omega_q t}b_q^\dagger(0)+e^{-i\omega_q t}b_{-q}(0)]\ ; \tag{2.8}$$

their correlation function gives the quantum fluctuation-dissipation relation for the system

$$\langle\hat{F}_m(t)\hat{F}_n(\tau)\rangle=\sum_q g_m^q g_n^{-q}\hbar^2\omega_q^2\{2\cos[\omega_q(t-\tau)]\times(\langle n_q\rangle+\tfrac{1}{2}) -i\sin[\omega_q(t-\tau)]\}\ ,$$
$$\lim_{T\to\infty}\langle\hat{F}_m(t)\hat{F}_n(\tau)\rangle=k_B T K_{mn}(t-\tau)\ , \tag{2.9}$$

where the $\langle\cdots\rangle$ indicates the trace with the equilibrium density operator of the free-phonon ($g=0$) bath at temperature T, $\langle n_q\rangle$ is the Bose distribution $[\exp(\hbar\omega_q/k_B T)-1]^{-1}$, and k_B is the Boltzmann constant. Using the coupling functions (2.4), the kernels take the form

$$K_{mn}(t)=\frac{g^2}{w}[J_{2(m-n-1)}(2\omega_B t)+2J_{2(m-n)}(2\omega_B t) +J_{2(m-n+1)}(2\omega_B t)]\ ,$$
$$K_{mn}(0)=\frac{g^2}{w}(\delta_{m,n+1}+2\delta_{m,n}+\delta_{m,n-1})\ , \tag{2.10}$$

where $J_\nu(z)$ is the Bessel function of the first kind of order ν.

III. COHERENT STATES

Most analyses of the Davydov model invoke in one way or another the Davydov ansatz for the state vector of the exciton-phonon system. The ansatz state is a tensor product of a one-exciton state and a product of phonon coherent states. To make progress in our analysis, we generalize the Davydov ansatz in a natural way:

$$|\psi_a(t)\rangle\equiv|\alpha(t)\rangle\otimes|\beta(t)\rangle\ , \tag{3.1a}$$

where

$$|\alpha(t)\rangle\equiv\exp\left[\frac{i}{\hbar}\sum_n[q_n(t)\hat{p}_n-p_n(t)\hat{q}_n]\right]|0\rangle\ , \tag{3.1b}$$

$$|\beta(t)\rangle\equiv\exp\left[\frac{i}{\hbar}\sum_n[Q_n(t)\hat{P}_n-P_n(t)\hat{Q}_n]\right]|0\rangle\ . \tag{3.1c}$$

This differs from the Davydov ansatz in that the vibron state $|\alpha(t)\rangle$ is defined here to be a coherent state rather than a definite number state as in the Davydov model. Although the mean number of vibron quanta may be essentially constant (slowly varying) in a time-dependent state (as we anticipate for states reasonably identified with solitons), vibron number is not conserved by the Takeno Hamiltonian, and thus the use of number-indefinite states greatly facilitates analysis. The factored form of the ansatz implies that our ansatz is not an exact solution of the Schrödinger equation of the system,[28] i.e.,

$$|\psi_a(t)\rangle\neq e^{-iHt/\hbar}|\psi_a(0)\rangle\ . \tag{3.2}$$

This approximation impacts our analysis of the Heisenberg equations obtained in the previous section when we make replacements

$$\langle\psi(0)|\hat{O}(t)|\psi(0)\rangle\to\langle\psi_a(t)|\hat{O}(0)|\psi_a(t)\rangle\ , \tag{3.3a}$$

$$\left\langle\psi(0)\left|\frac{d\hat{O}(t)}{dt}\right|\psi(0)\right\rangle\to\frac{d}{dt}\langle\psi_a(t)|\hat{O}(0)|\psi_a(t)\rangle\ . \tag{3.3b}$$

It is because of this approximation that it is desirable to integrate the exact Heisenberg equations as far as possible [as in (2.6)] before applying coherent-state methods. However, doing so requires that one analyze two-time correlation functions

$$\langle\psi(0)|\hat{A}(t_1)\hat{B}(t_2)|\psi(0)\rangle =\langle\psi(t_1)|\hat{A}(0)e^{-iH(t_1-t_2)/\hbar}\hat{B}(0)|\psi(t_2)\rangle \simeq\langle\psi_a(t_1)|\hat{A}(0)e^{-iH(t_1-t_2)/\hbar}\hat{B}(0)|\psi_a(t_2)\rangle \tag{3.4}$$

which are generally intractable even in the basis of coherent states. On the other hand, the factored approximation

$$\langle\psi(0)|\hat{A}(t_1)\hat{B}(t_2)|\psi(0)\rangle\approx\langle\psi_a(t_1)|\hat{A}(0)|\psi_a(t_1)\rangle \times\langle\psi_a(t_2)|\hat{B}(0)|\psi_a(t_2)\rangle \tag{3.5}$$

results in wieldable equations of motion; however, all the benefits of explicit operator integration are lost and (2.6) is rendered entirely equivalent to the unintegrated system (2.3). In this paper we forfeit the quantum corrections made available by the integrated form of the Heisenberg equations (2.6) and base our coherent-state analyses on the unintegrated system (2.3). It is our unproven view that this use of coherent states is less serious an approximation than corresponding coherent-state analysis of the Davydov model, since the lack of number conservation in the Takeno model assures finite-amplitude contributions from multiple-quantum states which become increasingly classical with increasing quantum number.

The remaining difficulty in applying coherent-state methods concerns the evaluation of expectation values. Elementary properties of coherent states give us the results[40,41]

$$\langle\psi_a(t)|\hat{q}_n|\psi_a(t)\rangle=q_n(t)\ , \tag{3.6a}$$

$$\langle\psi_a(t)|\hat{p}_n|\psi_a(t)\rangle=p_n(t)\ , \tag{3.6b}$$

$$\langle\psi_a(t)|\hat{Q}_n|\psi_a(t)\rangle=Q_n(t)\ , \tag{3.6c}$$

$$\langle\psi_a(t)|\hat{P}_n|\psi_a(t)\rangle=P_n(t)\ . \tag{3.6d}$$

However, for more general operator-valued functions $f\{\hat{q},\hat{p}\}$ Taylor expandable in the operators $\{\hat{q},\hat{p}\}$, it follows that

$$\begin{aligned}\langle\alpha(t)|f\{\hat{q},\hat{p}\}|\alpha(t)\rangle&=\langle\alpha(t)|f_N(\hat{q},\hat{p})|\alpha(t)\rangle\\&=f_N\{q(t),p(t)\}\ ,\end{aligned} \tag{3.7}$$

where f_N is the normal-ordered function associated with f and not f itself.[41] From this follow the relations

$$\frac{1}{i\hbar}\langle\alpha(t)|[\hat{q}_n,f\{\hat{q},\hat{p}\}]|\alpha(t)\rangle=\frac{\partial f_N\{q(t),p(t)\}}{\partial p_n(t)}\ , \tag{3.8a}$$

$$\frac{1}{i\hbar}\langle\alpha(t)|[\hat{p}_n,f\{\hat{q},\hat{p}\}]|\alpha(t)\rangle=-\frac{\partial f_N\{q(t),p(t)\}}{\partial q_n(t)}\ , \tag{3.8b}$$

which are analogous to Hamilton's equations. The distinction between f and f_N is a quantum effect. One can show that

$$f_N\{q(t),p(t)\}=f\{q(t),p(t)\}(1+O\{N^{-1}\})\ , \tag{3.9}$$

where N is the average number of quanta in the relevant mode. Thus, f and f_N coincide in the correspondence limit $N\to\infty$, and Eqs. (3.8) become Hamilton's equations. One consequence of this is that a large-N system prepared in a coherent state will persist in that state with high accuracy for long times. However, the distinction, and hence the error, can be significant when f is anharmonic and only small numbers of quanta are involved. Thus, in the present context we have

$$\langle\psi_a(t)|v(\hat{q}_n)|\psi_a(t)\rangle=v_N[q_n(t)]\ , \tag{3.10a}$$

$$\langle\psi_a(t)|g(\hat{q}_n)|\psi_a(t)\rangle=g_N[q_n(t)]\ . \tag{3.10b}$$

Applying (3.3), (3.6), and (3.10) to the (general) Takeno Hamiltonian (1.3) the Heisenberg vibron equations can be translated into equations of motion for coherent state amplitudes, or equivalently, displacement and momentum expectation values:

$$\dot{q}_n(t)=\frac{p_n(t)}{m}\ , \tag{3.11a}$$

$$\begin{aligned}\dot{p}_n(t)=&-\frac{\partial v_N[q_n(t)]}{\partial q_n(t)}+2\sum_m L_{nm}q_m\\&-g^{-1}f_n(t)\frac{\partial g_N[q_n(t)]}{\partial q_n(t)}\\&-g^{-2}\sum_m\int_0^t d\tau\,\dot{K}_{nm}(t-\tau)g_N[q_m(\tau)]\\&\times\frac{\partial g_N[q_n(t)]}{\partial q_n(t)}\ .\end{aligned} \tag{3.11b}$$

[The scaling of terms in (3.11) by inverse powers of the coupling constant g is a notational convenience only.] The fluctuating coefficient $f_n(t)$ appears when lattice variables are eliminated by integrating (2.3c) and is constructed from the initial-value contributions arising from (2.3c) or (2.5) after applying coherent states.

Equations of the same form would be obtained from a classical derivation, with the exception that the normal-ordered functions v_N and g_N would be the "classical" functions v and g. In the quadratic Takeno model, $v\neq v_N$ and $g\neq g_N$; however, in each case the difference is only an additive constant. In the case of v and v_N, the constant acts only to shift the total energy and hence is irrelevant. In the case of g and g_N, the constant introduces a term which is generally sensitive to volume dilation; however, this term vanishes in our case due to the assumed translational invariance.

In order to obtain solitary-wave solutions appropriate for the description of long-wavelength excitations, we require the transcription of (3.11) into continuum form. We carry out the continuum limit by reparametrizing the discrete equations in terms of bulk parameters which remain finite as $l\to 0$ and using normal-mode relations to define the continuum-field variables. Thus we define the continuum parameters and auxiliary functions as follows:

$$\eta=\frac{M}{l},\quad \mu=\frac{m}{l} \tag{3.12a}$$

$$\zeta=wl,\quad v_a=\sqrt{\zeta/\eta} \tag{3.12b}$$

$$\begin{aligned}&\omega(k)=[\omega^2(0)+k^2v_f^2]^{1/2}\ ,\\&\omega(0)=\left[\omega_v^2-\frac{4L}{m}\right]^{1/2}\ ,\end{aligned} \tag{3.12c}$$

$$L_{nm}=L(\delta_{n,m+1}+\delta_{n,m-1})\to 2L+Ll^2\frac{\partial^2}{\partial x^2}\ , \tag{3.12d}$$

$$\Box\equiv v_f^2\frac{\partial^2}{\partial x^2}-\frac{\partial^2}{\partial t^2}\ , \tag{3.12e}$$

$$K_{mn}(t)\to K(x,y,t)=\frac{2g^2}{\zeta}[\delta(x-y+v_at)+\delta(x-y-v_at)]\ , \tag{3.12f}$$

$$f_n(t)\to f(x,t)=g\left[\frac{\partial Q(y,0)}{\partial y}+\frac{P(y,0)}{\eta v_a}\right]_{y=x+v_at}+g\left[\frac{\partial Q(y,0)}{\partial y}-\frac{P(y,0)}{\eta v_a}\right]_{y=x-v_at}\ . \tag{3.12g}$$

Then, in the continuum limit, Eqs. (3.11) can be rewritten as

$$\Box q(x,t)=\frac{1}{\mu}\left[\frac{\partial v_N[q(x,t)]}{\partial q(x,t)}-\frac{4L}{l}q(x,t)\right]+\frac{1}{\mu g^2}\int_{-\infty}^{\infty}dy\int_0^t d\tau\,\dot{K}(x,y,t-\tau)g_N[q(y,\tau)]\frac{\partial g_N[q(x,t)]}{\partial q(x,t)}+\frac{1}{\mu g}f(x,t)\frac{\partial g_N[q(x,t)]}{\partial q(x,t)}\ . \tag{3.13}$$

IV. APPROXIMATE SOLUTIONS

The results of the foregoing sections establish a framework within which one may address diverse questions. In this section we focus on finding approximate solutions. Since no useful solution of the dynamical equations appears accessible in the presence of thermal noise, we limit our discussion to temperatures sufficiently low that the role of thermal fluctuations may be neglected. It is important to note that in general the "fluctuation" $f(x,t)$ appearing in (3.13) contains both systematic and random contributions. If a coherent structure such as a soliton exists in the system at the initial time, the initial coordinates of the medium reflect the superposition of a coherent deformation and thermal noise

$$f(x,t)=f^{\rm sol}(x,t)+f^{\rm th}(x,t)\ . \tag{4.1}$$

At sufficiently low temperatures, the thermal noise $f^{\rm th}(x,t)$ may be neglected and $f(x,t)$ contains only the coherent deformation $f^{\rm sol}(x,t)$.

For the sake of simplicity, let us first consider the quadratic Takeno model in which both the local oscillator potential $v(q)$ and the coupling function $g(q)$ are quadratic functions of q. For the quadratic Takeno model, Eq. (3.15) can be simplified

$$\Box q(x,t)=\omega^2(0)q(x,t)+\frac{2}{\mu}f^{\rm sol}(x,t)q(x,t)+\frac{G(0)}{\mu}\int_0^t d\tau\left[\frac{\partial}{\partial t}q^2(y,\tau)\bigg|_{y=x+v_a(t-\tau)}\right]q(x,t)+\frac{G(0)}{\mu}\int_0^t d\tau\left[\frac{\partial}{\partial t}q^2(y,\tau)\bigg|_{y=x-v_a(t-\tau)}\right]q(x,t)\ , \tag{4.2}$$

wherein $\omega(0)$ is the lowest frequency of the vibron band. For later convenience, we also define

$$G(v)\equiv\gamma_a^2\frac{4g^2}{\zeta},\quad \gamma_a\equiv\frac{1}{(1-v^2/v_a^2)^{1/2}}\ ,\qquad \gamma_f\equiv\frac{1}{(1-v^2/v_f^2)^{1/2}}\ . \tag{4.3}$$

Rather than attempting the general solution of (4.2), we look for traveling-wave solutions. Let us consider a modulated carrier wave of the form

$$q(x,t)=\phi[\kappa(x-vt)]\cos[kx-\tilde{\omega}(k)t]\ , \tag{4.4}$$

in which $\phi[\kappa(x-vt)]$ is a real envelope function whose width is given by κ^{-1}. The carrier wave frequency $\tilde{\omega}(k)$ appropriate to a given k will differ, in general, from the corresponding frequency $\omega(k)$ of the linear system.

On manipulation of the integrals in (4.1), one finds that the character of the integrands is controlled by the di-

mensionless parameters

$$R_{\pm}=\left|\frac{kv_a\pm\tilde{\omega}(k)}{\kappa(v_a\pm v)}\right| . \tag{4.5}$$

[Hereafter we drop the subscript $(\pm)$ for convenience.] When $R\gg1$, there are many carrier wave oscillations modulating the envelope function so that one may accurately approximate the integrals using the rotating-wave approximation (RWA)

$$\begin{aligned}q^2(y,\tau)&=\phi^2[\kappa(y-v\tau)]\cos^2[ky-\tilde{\omega}(k)\tau]\\&\approx\tfrac{1}{2}\phi^2[\kappa(y-v\tau)] .\end{aligned} \tag{4.6}$$

The condition $R\gg1$ includes limits which are easily visualized. [We assume that $v\ll v_a$ and $\tilde{\omega}(k)\neq kv_a$.] First we consider the limit in which the phase velocity is greater than the sound speed, so that our wave packets are constructed from frequencies near the center of the Brillouin zone. In this limit, the condition $(R\gg1)$ is the same as the condition $\tilde{\omega}(k)\gg\kappa v_a$, which requires that many carrier wave oscillations elapse during the time required for a sound wave to propagate across the envelope. The averaging effected by the RWA is then primarily of a temporal character. The second limit is that in which the phase velocity is less than the sound speed, so that our wave packets are constructed from frequencies in the outer part of the Brillouin zone. In this limit, the condition $(R\gg1)$ is the same as the condition $k\gg\kappa$, which requires that the envelope span many wavelengths of the carrier. The averaging effected by the RWA is then primarily of a spatial character. Thus the integral terms in (4.2) can be evaluated, and (4.2) can be rewritten as

$$\begin{aligned}\Box q(x,t)=\omega^2(0)q(x,t)&-\frac{G(v)}{\mu}\phi^2[\kappa(x-vt)]q(x,t)+\frac{2}{\mu}f^{\rm sol}(x,t)q(x,t)\\&+\frac{G(0)}{2\mu}\left[\frac{v_a}{v_a-v}\phi^2[\kappa(x-v_at)]+\frac{v_a}{v_a+v}\phi^2[\kappa(x+v_at)]\right]q(x,t) .\end{aligned} \tag{4.7}$$

For *preformed solitons* the coherent fluctuation $f^{\rm sol}(x,t)$ has the form required to cancel the traveling potentials proportional to

$$(v_a\pm v)^{-1}\phi^2[\kappa(x\pm v_at)] ,$$

so we obtain the equation

$$\Box q(x,t)=\omega^2(0)q(x,t)-\frac{G(v)}{\mu}\phi^2[\kappa(x-vt)]q(x,t) , \tag{4.8}$$

which has solutions of the form

$$q(x,t)=\phi_0\,\mathrm{sech}[\kappa(x-vt)]\cos[kx-\tilde{\omega}(k)t] , \tag{4.9a}$$

accompanied by deformations

$$Q(x,t)=-\gamma_a^2\frac{g}{\kappa\zeta}\phi_0^2\tanh[\kappa(x-vt)] . \tag{4.9b}$$

The five parameters ϕ_0, κ, v, k, and $\tilde{\omega}(k)$ are constrained by three relations (see Appendix A). First, the usual relation between group and phase velocities continues to hold

$$v\left[\frac{\tilde{\omega}(k)}{k}\right]=v_f^2 ; \tag{4.10a}$$

second, the width of the envelope is constrained by

$$\kappa=\left[\frac{\omega^2(k)-\tilde{\omega}^2(k)}{v_f^2-v^2}\right]^{1/2} ; \tag{4.10b}$$

third, ϕ_0 is constrained by the boundary conditions [cf. (7.7)] that select the solitary-wave form (4.9a) over the numerous nonlinear wave trains which may be found for (4.8),

$$\phi_0=\left[\frac{2\mu[\omega^2(k)-\tilde{\omega}^2(k)]}{G(v)}\right]^{1/2} . \tag{4.10c}$$

If one proceeds in this way, one may find for every pair (ϕ_0,k) (for example) a value for the total energy

$$\tilde{E}(\phi_0,k)=\langle\psi_a(t)|\hat{H}_{\rm Takeno}|\psi_a(t)\rangle . \tag{4.11}$$

For a number of purposes, this is a satisfactory state in which to leave these results since ϕ_0 and k determine a unique solution and its energy. For a number of purposes, however, the amplitude ϕ_0 is too derived a quantity to provide the quality of answer desired. For example, it is important to understand how the solitary-wave energy splits away from the linear-wave energy as vibron-phonon coupling is turned on. Equation (4.11) provides an answer; however, the answer is incomplete because it depends on ϕ_0 which should itself vary with changes in coupling strength in a manner as yet undetermined. What is needed is a quantifiable property of both linear and solitary waves which is invariant under variations in coupling strength and which has a sensible quantum interpretation. (In the theory of Davydov, this implicit need is filled by the number-conserving property of the Fröhlich Hamiltonian; not only is exciton number conserved in time, it is independent of coupling strength as well.)

The adiabatic invariance of the action in classical mechanics is manifested in quantum mechanics in the property of quantum systems that energy eigenstates and

eigenvalues repond to slow variations of Hamiltonian parameters *in concert,* such that the distribution of quanta over energy levels does not change. That is, occupation numbers of energy eigenstates inherit the adiabatic invariance of the actions from which they are derived. Our solitary-wave solutions are not connected with pure eigenstates in the linear limit, but with vibron coherent states having a certain mean number n of vibron quanta distributed over the number states of a particular normal mode. As vibron-phonon coupling is turned on slowly, the energy level spacings and the character of the *number states* should change while n and its associated distribution remain fixed. We wish to exploit this invariance to eliminate ϕ_0 and express all results in terms of n and k.

To do this precisely, of course, would be to completely solve the problem. Instead, we observe that the amplitude ϕ_0 of a vibron coherent state in the normal mode k having a mean number of quanta n is given by

$$\phi_0=\left[\frac{n\hbar}{2\mu\omega(k)L}\right]^{1/2} . \tag{4.12a}$$

We assume that in the presence of vibron-phonon coupling the amplitude is given by

$$\phi_0=\left[\frac{n\hbar\kappa}{\mu\tilde{\omega}(k)}\right]^{1/2} , \tag{4.12b}$$

where n is the mean number of quanta in the mode which is assumed to be invariant under variations in coupling strength. κ^{-1} is proportional to the width of the soliton envelope; however, $\kappa\rightarrow O\{L^{-1}\}$ in the weak-coupling limit, where L is the size of the system, thus maintaining formal continuity with the normal modes of the linear system. In the absence of coupling $\tilde{\omega}(k)$ is the linear frequency $\omega(k)$; however, increasing coupling causes $\tilde{\omega}(k)$ to redshift away from $\omega(k)$ and split into a band due to the implicit dependence of $\tilde{\omega}(k)$ on the mean number of quanta n. What is being split is not an energy degeneracy in the usual sense, rather it is the degeneracy of the energy per quantum with respect to the number of quanta; that is, unlike the normal modes of a linear system, the energy required to increase the number of quanta in one of our nonlinear modes depends on the number of quanta already in the mode. The present situation is similar in this respect to the quantization of bound, anharmonic oscillations for which the softening of potentials with increasing amplitude results in energy level spacings which decrease with increasing quantum number. This same similarity alerts us to the nonequivalence of $n\hbar\tilde{\omega}(k)$ and the energy except in the linear limit. Beyond maintaining formal continuity with the linear limit, (4.12b) is the simplest assumption we have found which allows a sensible interpretation of the virial theorem (see Appendix A).

For convenience we now define a dimensionless coupling constant incorporating the mean number of quanta

$$\sigma=\frac{n\hbar G(0)}{\mu^2 v_f\omega^2(0)} , \tag{4.13}$$

in terms of which we express the relation which determines the k dependence of $\tilde{\omega}(k)$

$$[\omega^2(k)-\tilde{\omega}^2(k)][\tilde{\omega}^2(k)-k^2v_f^2]=\tfrac{1}{4}\gamma_a^4\sigma^2\omega^4(0) . \tag{4.14}$$

The properties of the solutions (4.9a) are most clearly apparent in the limit of a large velocity of sound. We momentarily limit our discussion to systems for which $v_f<v_a$ so that we may safely assume $v\ll v_a$, and hence $\gamma_a\approx 1$. For such systems the k dependence of the various quantities of interest is particularly simple. Equation (4.14) yields two branches of solutions, which we distinguish with subscripts $(\pm)$,

$$\tilde{\omega}_\pm(k)=[\tilde{\omega}_\pm^2(0)+k^2v_f^2]^{1/2} , \tag{4.15a}$$

$$\tilde{\omega}_+(0)=\omega(0)\cos(\tfrac{1}{2}\sin^{-1}\sigma) , \tag{4.15b}$$

$$\tilde{\omega}_-(0)=\omega(0)\sin(\tfrac{1}{2}\sin^{-1}\sigma) , \tag{4.15c}$$

$$v_\pm\left[\frac{\tilde{\omega}_\pm(k)}{k}\right]=v_f^2 , \tag{4.15d}$$

$$\kappa_\pm=\frac{\tilde{\omega}_\pm(k)}{v_f}[\tan(\tfrac{1}{2}\sin^{-1}\sigma)]^{\pm 1} , \tag{4.15e}$$

$$\tilde{E}=n\hbar\tilde{\omega}_\pm(k)\{1+\tfrac{1}{3}[\tan(\tfrac{1}{2}\sin^{-1}\sigma)]^{\pm 2}\} , \tag{4.15f}$$

where (4.15f) is computed according to (4.11) (cf. Appendix A and Table I). The general behaviors of these quantities are indicated in Figs. 2 and 3. Beyond the "critical" coupling $\sigma=1$ the carrier wave frequencies become complex. At critical coupling we find

$$\tilde{\omega}_c(k)\equiv\tilde{\omega}_\pm(k)|_{\sigma=1} , \tag{4.16a}$$

$$\kappa_c\equiv\kappa_\pm|_{\sigma=1}=\frac{\tilde{\omega}_c(k)}{v_f} , \tag{4.16b}$$

and

$$\tilde{E}_c\equiv\tilde{E}|_{\sigma=1}=\tfrac{4}{3}n\hbar\tilde{\omega}_c(k) . \tag{4.16c}$$

We note that while the above quantities converge to the same values at *critical* coupling, strong differences appear as the *weak*-coupling limit is approached; namely the total energy of any lower-branch $(-)$ solution diverges while upper-branch $(+)$ energies approach the proper linear energies, and the width of any lower-branch solution tends to zero while upper-branch solutions broaden toward plane waves.

While the various solutions corresponding to these parameters appear on an equal footing as solutions of the approximate equation (4.8), they do not all approximate the solutions of (4.2) with equal accuracy. The overriding condition for the validity of (4.8) and the approximate solutions (4.9a) is the rotating-wave condition $R\gg 1$. We now render this condition more specific by considering outer-zone $[\tilde{\omega}(k)<kv_a]$ solutions and inner-zone $[\tilde{\omega}(k)>kv_a]$ solutions separately.

In the outer zone, the condition $R\gg 1$ reduces to the condition $k\gg\kappa$. Using (4.15d) and (4.15e), we find that the validity of the RWA depends on the validity of the inequality

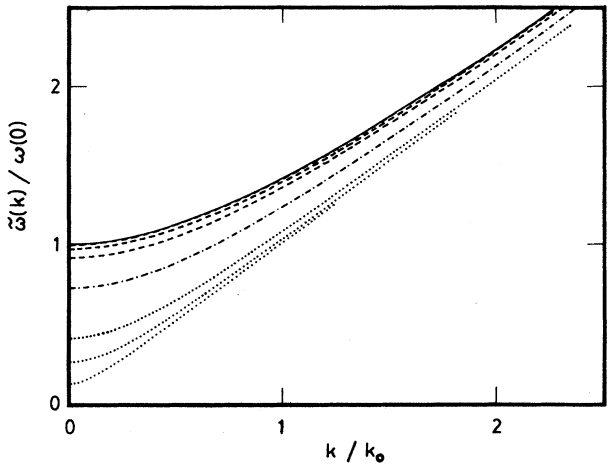

FIG. 2. Carrier wave frequency $\tilde{\omega}_{\pm}(k)$ in the limit of infinite acoustic sound speed. Solid line (——), linear limit ($\sigma=0$); dashed line (— — —), $\tilde{\omega}_{+}(k)$ for $\sigma=\frac{1}{4},\frac{1}{2},\frac{3}{4}$; chain dotted (—·—·—·), $\tilde{\omega}_{c}(k)$; dotted (· · · ·), $\tilde{\omega}_{-}(k)$ for $\sigma=\frac{3}{4},\frac{1}{2},\frac{1}{4}$. Note that for $\sigma=\frac{1}{4}$, $\tilde{\omega}_{+}(k)$ lies too close to $\omega(k)$ to be resolved in this graph.

$$\frac{v_{\pm}}{v_f} \gg [\tan(\tfrac{1}{2}\sin^{-1}\sigma)]^{\pm 1} . \tag{4.17}$$

Upper-branch (+) solutions are thus generally valid in the outer zone, provided that coupling is sufficiently weak. On the other hand, since $v<v_f$ for *all* solutions, we find that (4.17), and hence the RWA, cannot be satisfied by *any* lower-branch (−) solution, regardless of coupling strength.

In the inner zone, the condition $R\gg 1$ reduces to the condition $\tilde{\omega}(k)\gg\kappa v_a$. Using (4.15e), we find that the validity of the RWA depends on the validity of the inequality

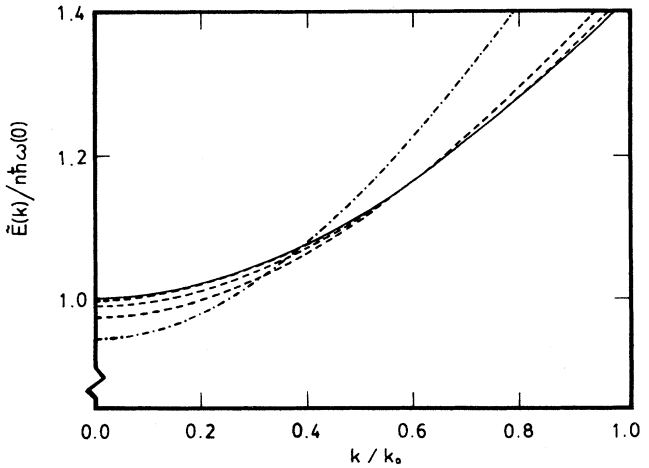

FIG. 3. Total system energy in the solitary-wave state $\tilde{E}(k)$ in the limit of an infinite acoustic sound speed. Solid line (——), linear limit ($\sigma=0$); dashed line (— — —), upper branch for $\sigma=\frac{1}{4},\frac{1}{2},\frac{3}{4}$; chain dotted (—·—·—·), critical coupling ($\sigma=1$). Note that although not plotted, the lower branch energy is higher than the upper branch energy and is higher than the linear energy in most cases.

$$\frac{v_f}{v_a} \gg [\tan(\tfrac{1}{2}\sin^{-1}\sigma)]^{\pm 1} . \tag{4.18}$$

Upper branch (+) solutions are thus generally valid in the inner zone, provided that coupling is sufficiently weak. On the other hand, for systems having $v_f<v_a$ (such as we consider), (4.18) and hence the RWA cannot be satisfied by *any* lower-branch (−) solution, regardless of coupling strength.

One can see the effect a finite-sound speed has on the above results simply by reintroducing the acoustic Lorentz factor, replacing σ by $\gamma_a^2\sigma$. The bounds (4.17) and (4.18) (with σ replaced by $\gamma_a^2\sigma$) which invalidate lower-branch solutions continue to hold for finite-sound speeds greater than the free-vibron speed, with the principal consequence of a finite-sound speed being that weaker coupling is required at higher k values in order for solutions to remain valid. However, if the sound speed is less than the free-vibron speed, then there is no outer zone, and only the bound (4.18) is relevant. The inequality (4.18) does not strictly exclude *all* of the lower branch; however, since part of the lower branch *is* excluded, and since no lower branch solution is valid in the weak-coupling limit, we interpret (4.18) as continuing to invalidate all lower-branch solutions.

The total energy (4.11) can be written in the form (see Appendix A)

$$\tilde{E}=\frac{n\hbar\tilde{\omega}(k)}{3\gamma_f^2}\left[2(\gamma_f^2-\gamma_a^2+1)+\frac{\gamma_f^2+2\gamma_a^2-2}{[\cos(\frac{1}{2}\sin^{-1}\gamma_a^2\sigma)]^2}\right] . \tag{4.19}$$

For small soliton speeds, $\tilde{E}$ can be written as

$$\tilde{E}=E_{\rm vib}-E_{\rm bind}+\tfrac{1}{2}m_{\rm sol}^{T}v^2 , \tag{4.20}$$

where $E_{\rm vib}$ is defined as the bare vibron energy at $k=0$, i.e., the $v=0$ vibron energy in the limit $\sigma\to 0$. $E_{\rm bind}$ is the binding energy and $m_{\rm sol}^{T}$ is the effective mass of the vibron soliton. $E_{\rm vib}$, $E_{\rm bind}$, and $m_{\rm sol}^{T}$ are given by

$$E_{\rm vib}=n\hbar\omega(0) , \tag{4.21a}$$

$$E_{\rm bind}=\tfrac{1}{3}\{3-2\cos(\tfrac{1}{2}\sin^{-1}\sigma) -[\cos(\tfrac{1}{2}\sin^{-1}\sigma)]^{-1}\}n\hbar\omega(0) , \tag{4.21b}$$

$$m_{\rm sol}^{T}=nm^{T}\left[[\cos(\tfrac{1}{2}\sin^{-1}\sigma)]^{-1} -\frac{2}{3}\left[1+\frac{v_f^2}{v_a^2}\right]\tan^2(\tfrac{1}{2}\sin^{-1}\sigma)\right] . \tag{4.21c}$$

We note that the maximum binding energy is obtained at the critical coupling $\sigma=1$

$$E_{\rm bind}|_{\sigma=1}=\tfrac{1}{3}(3-2\sqrt{2})n\hbar\omega(0) . \tag{4.22}$$

In the weak-coupling limit, the binding energy comes into agreement with the result for the Davydov model[42]

$$E_{\rm bind}\approx\frac{\sigma^2}{24}n\hbar\omega(0) , \tag{4.23}$$

and the effective mass can be simplified

$$m_{\rm sol}^{T} \approx \frac{n\hbar\omega(0)}{v_f^2}\left[1-\frac{\sigma^2}{24}\left[1-4\frac{v_f^2}{v_a^2}\right]\right] . \tag{4.24}$$

This weak-coupling relation offers an interesting manifestation of a distinction between the Davydov and Takeno models noted in the introduction. In order to recover Davydov's effective mass, we must assert the inequality $v_f \gg v_a$, whereupon

$$m_{\rm sol}^{T} \approx \frac{n\hbar\omega(0)}{v_f^2}\left[1+\frac{\sigma^2}{6}\frac{v_f^2}{v_a^2}\right] , \tag{4.25}$$

which agrees with Davydov's result.[42] On the other hand, when $v_f < \frac{1}{2}v_a$, as is the case in many narrow-band systems, the effect of vibron-phonon coupling is to *reduce* the effective mass, rather than increase it as in (4.25).

The general behavior of the carrier wave frequency $\tilde{\omega}(k)$ and the total energy $\tilde{E}(k)$ are indicated in Figs. 4 and 5, respectively, for a case in which the speed of sound v_a is not excessively larger than the free vibron speed v_f. Two interesting consequences of a finite-sound speed are the appearance of an ultraviolet wave-vector cutoff $k_{\rm max}$ and a maximum speed $v_{\rm max}$ other than the free vibron speed v_f. We observe that the carrier wave frequencies $\tilde{\omega}$ are real only if $\gamma_a^2\sigma < 1$. The condition $\gamma_a^2\sigma = 1$ provides extreme values which demark the maximum values various parameters may assume; thus, we find generally

$$v_{\rm max} = \begin{cases} v_f, \quad 0 \le \sigma \le 1-\min\left\{1, \dfrac{v_f^2}{v_a^2}\right\} & \text{(4.26a)} \\ v_a\sqrt{(1-\sigma)}, \quad 1 \ge \sigma \ge 1-\min\left\{1, \dfrac{v_f^2}{v_a^2}\right\} & \text{(4.26b)} \end{cases}$$

$$k_{\rm max} = \begin{cases} \infty, \quad 0 \le \sigma \le 1-\min\left\{1, \dfrac{v_f^2}{v_a^2}\right\} & \text{(4.27a)} \\ \dfrac{\omega(0)}{\sqrt{2}v_f}\dfrac{v_{\rm max}}{(v_f^2-v_{\rm max}^2)^{1/2}}, \\ \qquad 1 \ge \sigma \ge 1-\min\left\{1, \dfrac{v_f^2}{v_a^2}\right\} . & \text{(4.27b)} \end{cases}$$

One must question whether the appearance of a finite $k_{\rm max}$ is an artifact of our rotating-wave approximation. We have no physical arguments to support the existence of an ultraviolet cutoff. If such cutoffs are physically meaningful, they should be associated with a resonance between the vibron and phonon systems, and there is no physical resonance which can be clearly identified as being responsible for the indicated features. In the absence of further clarification of the possible role of a finite $k_{\rm max}$, the conservative interpretation of (4.26) and (4.27) takes the form of a weak-coupling condition

$$\sigma < 1-v_f^2/v_a^2 . \tag{4.28}$$

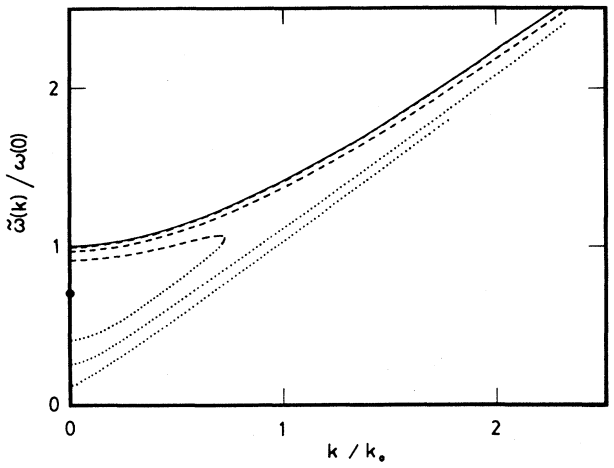

FIG. 4. Carrier wave frequency $\tilde{\omega}_{\pm}(k)$ for a finite acoustic sound speed, $v_a = \sqrt{2}v_f$. Solid line (——), linear limit ($\sigma = 0$); dashed line (— — —), $\tilde{\omega}_{+}(k)$ for $\sigma = \frac{1}{4}, \frac{1}{2}, \frac{3}{4}$; bullet (●), critical coupling; dotted (· · ·), $\tilde{\omega}_{-}(k)$ for $\sigma = \frac{3}{4}, \frac{1}{2}, \frac{1}{4}$. Note that for $\sigma = \frac{1}{4}$, $\tilde{\omega}_{+}(k)$ lies too close to $\omega(k)$ to be resolved in this graph.

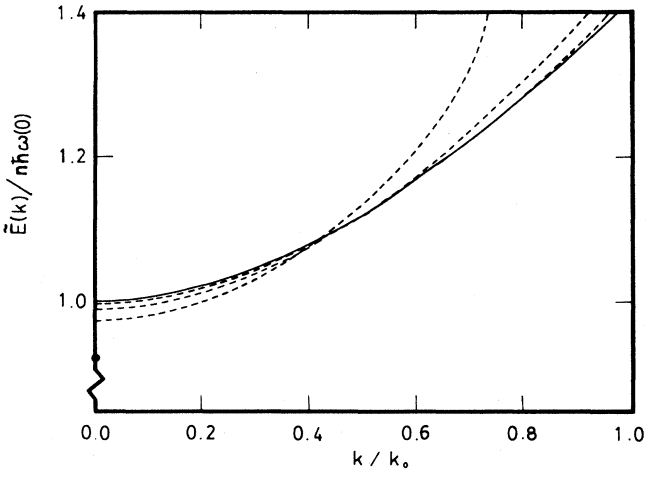

FIG. 5. Total system energy in the solitary wave state, $\tilde{E}(k)$, for a finite acoustic sound speed, $v_a = \sqrt{2}v_f$. Solid line (——), linear limit ($\sigma = 0$); dashed line (— — —), "upper branch" for $\sigma = \frac{1}{4}, \frac{1}{2}, \frac{3}{4}$; bullet (●), critical coupling ($\sigma = 1$). Note that although not plotted, the lower-branch energy is higher than the upper-branch energy and is higher than the linear energy in most cases.

V. INSTABILITIES

We encounter several instabilities in our analysis of the quadratic Takeno model. Perhaps the most obvious is the existence of a critical value of the coupling ($\sigma=1$) beyond which the oscillation frequencies of our modulated carrier wave solutions become complex. One must question whether this critical behavior is a property to be found in real systems, or whether it is perhaps unique to the quadratic Takeno model, or whether it is an artifact of our approximate analysis. That the behavior is not an artifact of our analysis can be seen easily by considering a nonlinear Klein-Gordon equation which is related to our integro-differential equations (4.2):

$$\Box q(x,t)=\omega^2(0)q(x,t)-\frac{G(v)}{\mu}q^3(x,t)\ . \tag{5.1}$$

Small-amplitude solutions of this equation are stable; however, should the amplitude $q(x,t)$ at any point exceed a critical value

$$q_c=\left[\frac{\mu\omega^2(0)}{G(v)}\right]^{1/2}\ , \tag{5.2}$$

an unbounded growth in amplitude ensues, resulting in a divergence which under most circumstances must be considered unphysical. The critical coupling ($\sigma=1$) encountered in the previous section occurs when the maximum value of the envelope function q_0 reaches the critical amplitude q_c. Thus we assert that the critical values of the various parameters we have found are not artifacts of our approximate analysis, but mark true critical features of the starting model.

The instability of the dynamics at large amplitude raises difficulties for the practical application of the quadratic Takeno model. Specifically, the spatial and temporal uniformity of the small-amplitude condition [$q(x,t)<q_c$ for all x and t] renders analysis of finite-temperature systems problematic since the very nature of thermal fluctuations assures that the critical amplitude will be attained somewhere in the system in a finite period of time. Whether such an event poses a problem in a specific application will depend on the particular parameter values relevant to the application and the particular questions addressed.

A second instability can be found if one notes that in general the energy of our solitary-wave solutions is *not* less than that of corresponding linear (plane) waves for all k. The crossing of the linear and nonlinear energies occurs at a wave vector $k^*\in(k_1^*,k_0^*)$ such that

$$k_0^*\equiv\lim_{\gamma_a^2\sigma\to 0}k^*=\frac{\tilde{\omega}_c(0)}{v_f}\ , \tag{5.3a}$$

$$\tilde{\omega}(k_0^*)=\sqrt{3}\tilde{\omega}_c(0)\ , \tag{5.3b}$$

$$k_1^*\equiv\lim_{\gamma_a^2\sigma\to 1}k^*=(\tfrac{2}{5})^{1/2}\frac{\tilde{\omega}_c(0)}{v_f}\ , \tag{5.4a}$$

$$\tilde{\omega}(k_1^*)=(\tfrac{7}{5})^{1/2}\tilde{\omega}_c(0)\ . \tag{5.4b}$$

Thus, all linear (plane) waves having wave vectors $k>k_0^*$ have energies lower than the corresponding solitary-wave solutions we have found in Sec. IV. On the other hand, all solitary waves having wave vectors $k<k_1^*$ have energies lower than corresponding linear waves. Between k_1^* and k_0^* the fraction of solitary waves having energies lower than corresponding linear waves varies smoothly from 1 to 0. These energy relationships suggest that short-wavelength linear waves and broad, long-wavelength solitary waves dominate the spectral decomposition of a general state.

We interpret the phenomenon giving rise to k_0^* as the well-known Benjamin-Feir instability.[43–45] The usual explanation of the Benjamin-Feir instability is given in terms of complex-amplitude wave trains in weakly nonlinear dispersive media. Plane waves are found to be stable with respect to short-wavelength perturbations and unstable with respect to long-wavelength perturbations. Since our equations of motion yield real solutions, every complex-amplitude wave train coexists with its complex conjugate and hence experiences a perturbation having the same wavelength as the real carrier wave. Thus, each real plane wave solution perturbs itself in the sense of Benjamin and Feir. On the basis of such an argument, one should anticipate that short-wavelength ($k>k^*$) plane waves should be stable and that long-wavelength ($k<k^*$) plane waves should be unstable. The reversed energy relations we find above and below k^* can be interpreted as a mechanical realization of this generic property of nonlinear wave equations.

The rotating-wave approximation on which our calculations are based requires that the phase velocity $\tilde{\omega}(k)/k$ not be too close to the speed of sound v_a. Moreover, the Lorentz factor γ_a explicitly requires that the group velocity not be too close to the speed of sound. The latter is easily understood in terms of the locking which must exist between the solitary-wave envelope and the comoving lattice deformation. Since the group velocity of lattice wave packets must be less than the speed of sound, locking to the envelope can exist only for vibron solitary waves having group velocities less than the speed of sound in the lattice. However, since our vibron solitary waves are modulated carrier waves, locking between the vibron and lattice coordinates can be complete only if locking between the individual carrier wave oscillations and the lattice motions can be maintained as well. Since the individual carrier oscillations travel with the phase velocity, this requires that the phase velocity be less than the speed of sound in the lattice. Clearly, in the inner zone locking to the full carrier wave is not possible; however, near $k=0$ the oscillations of the carrier wave are sufficiently rapid that the RWA is justified, and locking to the envelope is still possible. In the limit of an infinite speed of sound there is no inner zone, and complete locking between vibron and lattice coordinates can be faithfully maintained.

Thus, our solutions are valid provided the wave vector k is not too close to k_{RWA} defined by

$$\tilde{\omega}(k_{\mathrm{RWA}})=k_{\mathrm{RWA}}v_a\ . \tag{5.5}$$

This observation, together with the form of the dispersion polynomial (4.14), is suggestive of polariton behav-

ior;[46] however, several differences are important to note: First, in the polariton problem the hybridization of an exciton or optical phonon field with a photon field results in a two-branch polariton spectrum $\tilde{\omega}_{\pm}(k)$ in which the upper-branch frequencies $\tilde{\omega}_{+}(k)$ are *blue*shifted, unlike the *red*shifting of the carrier wave frequency we obtain. Second, as a linear problem, polariton energies are proportional to polariton frequencies $[\tilde{E}_{\pm}(k)=n\hbar\tilde{\omega}_{\pm}(k)]$, unlike the distinct behaviors we find for these quantities. Third, hybridization in the polariton problem results in level repulsion in the neighborhood of the intersection of the decoupled dispersion curves (at $k\approx k_{\mathrm{RWA}}$), whereas this apparent intersection is wholly featureless in our results. In all likelihood this latter distinction is an artifact of our rotating-wave approximation; it is reasonable to conjecture that the true dispersion curves are repelled from the point $\tilde{\omega}(k_{\mathrm{RWA}})=k_{\mathrm{RWA}}v_a$ and merge with the acoustic branch. It is possible that the physical resonance suggested by k_{RWA} is the phantom resonance which should be associated with $k_{\max}$; such a possibility would be consistent with the discussion of $k_{\max}$ above and would reconcile both difficulties. In any case, one should anticipate that for weak coupling the extent of the hybridization region in k space should be small and that our solutions and their associated spectra should be valid over most of the Brillouin zone and particularly near the zone center.

VI. QUASICONTINUA

When the mean number of vibron quanta is sufficiently large or the coupling between the excitation and the lattice is sufficiently strong, the soliton width κ^{-1} can become comparable to a lattice constant, and our continuum treatment may no longer faithfully reflect the dynamics in the discrete medium. Discreteness corrections can be introduced by means of a gradient expansion, wherein the leading correction is of second order in the lattice constant l and brings in a second spatial derivative. While these results allow a sense to be gained for the role played by the microstructure of real solids, one must be wary of overinterpreting extreme results; any large deviations from our continuum results demand careful scrutiny, since a large contribution from this first correction suggests a significant role may be played by higher-order corrections not taken into account.

Implementing the procedure of Ref. 18, we retain the leading discreteness correction and consider the augmented equations

$$\Box q(x,t)=\omega^2(0)q(x,t)+\frac{2}{\mu}f^{\mathrm{sol}}(x,t)q(x,t)+\frac{G(0)}{\mu}\int_0^t d\tau\left[\frac{\partial}{\partial t}\left[1+\frac{l^2}{4}\frac{\partial^2}{\partial y^2}\right]q^2(y,\tau)\Big|_{y=x+v_a(t-\tau)}\right]q(x,t)$$
$$+\frac{G(0)}{\mu}\int_0^t d\tau\left[\frac{\partial}{\partial t}\left[1+\frac{l^2}{4}\frac{\partial^2}{\partial y^2}\right]q^2(y,\tau)\Big|_{y=x-v_a(t-\tau)}\right]q(x,t)\ . \tag{6.1}$$

As in the previous section, we are interested in preformed solitary waves having the modulated carrier form (4.4). Implementing the RWA in the same way as in the previous section, we find the modified wave equation

$$\Box q(x,t)=\omega^2(0)q(x,t)-\frac{G(v)}{\mu}\left[\phi^2(x,t)+\frac{l^2}{4}\frac{\partial^2}{\partial x^2}\phi^2(x,t)\right]q(x,t)\ . \tag{6.2}$$

The rotating-wave criterion $R\gg 1$ is the same as in Sec. IV; however, the details of the particular validity conditions which follow from it will be modified since the relationships among the various parameters will be modified by discreteness corrections. The equation for the envelope function can be written in the same form as that of the modified nonlinear Schrödinger equation.[18] The envelope function can be found and characterized by a dimensionless discreteness parameter D which vanishes in the continuum limit, but may be large in a real solid (see Appendix B).

Although the envelope function can be found for arbitrary D, the envelope equation can be solved most easily in the limit $D\gg 1$, in which the solution approaches the form

$$q(x,t)=\begin{cases}\left[\dfrac{4n\hbar}{\pi l\mu\tilde{\omega}(k)}\right]^{1/2}\cos[l^{-1}(x-vt)]\cos[kx-\tilde{\omega}(k)t] & \text{for } |x-vt|\le\dfrac{\pi l}{2}\\ 0 \quad \text{for } |x-vt|\ge\dfrac{\pi l}{2}\ ,\end{cases} \tag{6.3}$$

$$Q(x,t)=\begin{cases}-\gamma_a^2\dfrac{n\hbar g}{\zeta\mu\tilde{\omega}(k)}\dfrac{1}{\pi}\{2l^{-1}(x-vt)+\sin[2l^{-1}(x-vt)]\} & \text{for } |x-vt|\le\dfrac{\pi l}{2}\\ -\gamma_a^2\dfrac{n\hbar g}{\zeta\mu\tilde{\omega}(k)}\mathrm{sgn}(x-vt) & \text{for } |x-vt|\ge\dfrac{\pi l}{2}\ .\end{cases} \tag{6.4}$$

(It should be noted that these limiting solutions cannot recover the continuum solutions, i.e., $l \to 0$ is not a valid limit.) Since the width of this extreme state is so small, the ballistic transport indicated by the characteristic $x - vt$ cannot accurately represent the motion of the excitation; indeed, on the basis of this and other considerations, one might expect such a highly localized state to be pinned to the lattice in a real system. In such a case only results for $v \approx 0$ would be meaningful, and so we limit our discussion accordingly. We retain sufficient k dependence as required to determine the relevant behaviors.

The carrier wave frequency is given by

$$[\omega^2(k) - \tilde{\omega}^2(k)]\tilde{\omega}(k) = \frac{2}{\pi}\sigma\omega^2(0) l^{-1} v_f \ . \tag{6.5}$$

The critical value of the coupling beyond which (6.5) admits no real solitons is greater than unity in the limit, as can be understood from the fact that the effect of the first discreteness corrections is to weaken the nonlinearity. For a given k the critical value of the coupling constant σ is

$$\sigma_c' = \frac{4}{3}\frac{\tilde{\omega}_c(0)}{\kappa v_f}\left[\frac{\omega(k)}{\omega(0)}\right]^2 . \tag{6.6}$$

The corresponding critical frequency is

$$\tilde{\omega}_c(k) = \frac{\omega(k)}{\sqrt{3}} \ . \tag{6.7}$$

Since we maintain that only solutions with $v \approx 0$ are meaningful in this limit, the meaningful critical values are those at $k = 0$

$$\sigma_c = \frac{\pi}{3\sqrt{3}}\left[\frac{l\omega(0)}{v_f}\right] \tag{6.8}$$

and the relevant critical frequency is $\tilde{\omega}_c(0)$. Generally, (6.5) admits two branches of solutions; however, arguments similar to those advanced in the previous section can be made which show the lower branch to be invalid under our approximations.

It is important to question how large D can be, both to check the internal consistency of our conclusions and to gain a sense for relevant material parameters. When $D \gg 1$, D is related to other parameters via

$$D = \frac{2}{\pi}\frac{\sigma}{\tilde{\omega}(k)}\frac{l\omega^2(k)}{v_f} \ . \tag{6.9}$$

From this it is easy to see that D is maximal at the critical coupling $\sigma = \sigma_c$. Thus, we define

$$D_{\max} \approx \frac{2}{3}\left[\frac{l\omega(0)}{v_f}\right]^2 , \tag{6.10}$$

in which we have neglected the k dependence of this quantity as being unmeaningful.

The total energy of the system is given by

$$\tilde{E}(0) = \left[\frac{7\tilde{\omega}(0)}{8\omega(0)} + \frac{\omega(0)}{8\tilde{\omega}(0)} + \frac{\omega(0)}{3\tilde{\omega}(0)D_{\max}}\right] n\hbar\omega(0) \tag{6.11}$$

(see Appendix B) which approaches the value

$$\tilde{E}_c(0) = \left[\frac{5}{4} + \frac{1}{D_{\max}}\right] n\hbar\tilde{\omega}_c(0) \tag{6.12}$$

at critical coupling. This critical energy is the minimum energy on the upper branch, but the global minimum actually falls on the excluded lower branch, a few percent below $\tilde{E}_c(0)$. The arguments of Sec. V suggest that this discrepancy may be due to the incompleteness of our discreteness correction, and that higher-order corrections may narrow the gap. In the limit $D_{\max} \to \infty$, $\tilde{E}_c(0)$ is approximately 76% of the continuum result (4.16c), corresponding to a binding energy 4–5 times larger than that found in the continuum calculation [cf. (4.22)]. However, D and $D_{\max}$ need not be excessively large for discreteness effects to enhance binding energies; sample calculations show that significant effects can appear for D and $D_{\max}$ in the range 2–5.

VII. THE GENERAL TAKENO MODEL

In light of the intrinsic instability of the quadratic Takeno Hamiltonian encountered for large-vibron amplitudes, we note here how our procedure may be generalized to obtain corresponding results for more general local potentials $v(\hat{q}_n)$ and coupling functions $g(\hat{q}_n)$. The more general form of the Takeno model is appropriate when the vibron potentials $v(\hat{q}_n)$ and the forces $g(\hat{q}_n)$ involve higher powers of $\hat{q}_n$, as is more realistic for real systems. A positive sixth power, for example, is the minimum addition necessary in order to quench the large-amplitude instability of the quadratic Takeno model.[47] Traveling-wave solutions in the form of (4.4) can still be obtained in this case. For the sake of simplicity, here we only discuss the case of the continuum limit, from Eq. (3.13). By implementing a more general rotating-wave approximation, we can obtain the following equation for *preformed solitons*

$$\Box q(x,t) = \frac{1}{\mu}\left[\frac{\partial v_N[q(x,t)]}{\partial q(x,t)} - \frac{4L}{l}q(x,t)\right] - \frac{G(v)}{\mu g^2}\frac{\overline{g_N(x,t)}}{g_N(x,t)}\frac{\partial g_N[q(x,t)]}{\partial q(x,t)} \ , \tag{7.1}$$

where $\overline{g_N(x,t)}$ is the average of $g_N[q(x,t)]$ over one or more vibron oscillations, as given by

$$\overline{g_N(x,t)} \equiv \sum_n^{\infty} \frac{1}{n!} g_N^{(n)} \overline{q^n(x,t)} = \sum_n^{\infty} \frac{1}{n!}\frac{(2n-1)!!}{2n!!} g_N^{(n)} \phi^{2n}(x - vt) \ , \tag{7.2a}$$

$$g_N^{(n)} \equiv \frac{\partial^n}{\partial q^n} g_N[q]\bigg|_{q=0} \ , \tag{7.2b}$$

such that $\overline{g_N(x,t)}$ is a function of $x - vt$ only.

With the assumption that both $v(q)$ and $g(q)$ are at least second order in q, we can factor a q from $\partial v[q]/\partial q$ and $\partial g[q]/\partial q$, and then similarly average the remainder, from which

$$\Box q(x,t) = u(x - vt) q(x,t) \ , \tag{7.3a}$$

where we have defined

$$u(x-vt)\equiv\frac{1}{\mu}\left[\overline{\left[\frac{\nu'(x,t)}{q(x,t)}\right]}-\frac{4L}{l}-\frac{G(v)}{g^2}\overline{g(x,t)\left[\frac{g'(x,t)}{q(x,t)}\right]}\right]. \quad (7.3b)$$

It should be noted that this procedure averages the antisymmetric part of ν_n and g_N to zero; thus, the procedure is best applied in systems having potentials and coupling functions of the appropriate symmetry. If we equate coefficients of $\cos[kx-\tilde{\omega}(k)t]$ and $\sin[kx-\tilde{\omega}(k)t]$, respectively, we find two independent relations, the first of which is (4.10a), and the second

$$\frac{\partial^2\phi(x)}{\partial x^2}=-\tilde{\omega}^2\phi(x)+\gamma_f^{-2}u[\phi(x)]\phi(x) \quad (7.4)$$

is the envelope equation we seek. Equations (4.5b) can be easily integrated once to obtain

$$E=\frac{1}{2}\left[\frac{\partial\phi}{\partial x}\right]^2+U(\phi), \quad (7.5)$$

where E is a constant of integration, and the "potential" $U(\phi)$ is defined by

$$U(\phi)\equiv\tfrac{1}{2}\tilde{\omega}^2\phi^2-\frac{1}{\gamma_f^2}\int_0^{\phi}d\phi'\,u(\phi')\phi'. \quad (7.6)$$

For solitary waves, the possible values of E are determined by the boundary conditions

$$\phi(\pm\infty)=0,\quad \frac{\partial}{\partial x}\phi(\pm\infty)=0. \quad (7.7)$$

In the specific case we have considered in this paper, $E=0$ was the only possible value; however, more than one value of E may be possible when $U(\phi)$ has multiple minima. For each value of E, it is possible that there may be more than one type of solution; these are found by solving the equation

$$U(\phi_0)=E \quad (7.8)$$

for the possible values of ϕ_0 and inverting the integral

$$x=\int_{\phi_0}^{\phi}d\phi'\frac{1}{\sqrt{2[E-U(\phi')]}}. \quad (7.9)$$

The typical solution does not satisfy boundary conditions (7.7) and takes the form of a traveling wave train, the character of which depends on the choice of E and the form of $U(\phi)$.

VIII. FINITE TEMPERATURE

At present we have no solutions for the finite-temperature case. We can, however, compare qualitative aspects of the role of thermal noise in the Davydov and Takeno models.

In the Davydov model, thermal noise drives the complex mode amplitude $\alpha(t)$ and is multiplicative:

$$\dot{\alpha}(t)=(\cdots)-i\frac{\hbar}{m\omega_v}f(t)\alpha(t). \quad (8.1)$$

Transformation to polar coordinates shows that the fluctuations drive only the *phase* of the oscillator, for which the noise is *additive*:

$$\dot{\theta}(t)=(\cdots)-i\frac{\hbar}{m\omega_v}f(t), \quad (8.2)$$

$$\dot{\rho}(t)=(\cdots). \quad (8.3)$$

Systems exhibiting noise of this type are commonly called Kubo oscillators.[48]

In the Takeno model, thermal fluctuations drive only the *momentum* of the oscillator, for which the noise is multiplicative:

$$\dot{q}(t)=(\cdots), \quad (8.4)$$

$$\dot{p}(t)=(\cdots)-2f(t)q(t). \quad (8.5)$$

Qualitative features of these two kinds of noise are represented in Fig. 6.

It is possible for a Kubo oscillator to explore the entire allowed energy surface (n=constant) through the action of fluctuations alone; that is, if the mechanics of the oscillator implied by the symbol $(\cdots)$ above is neglected, thermal fluctuations will nonetheless cause the oscillator to pass through all of its allowed states. For example, colored noise with a sufficiently long correlation time will sweep the phase of the oscillator through all four quadrants of phase space, allowing the oscillator to execute complete cycles under the influence of noise alone. White noise achieves the same result by a more tortuous path.

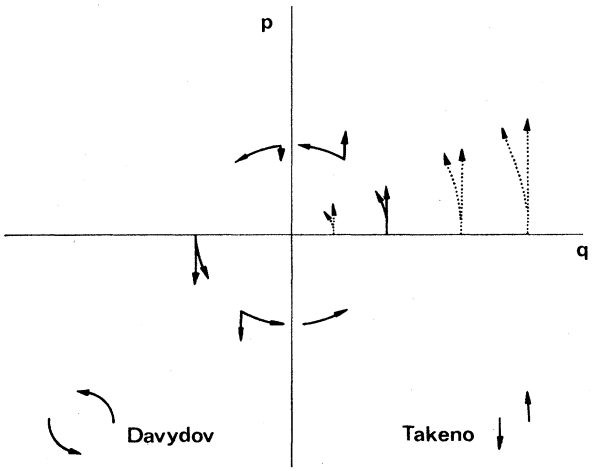

FIG. 6. Fluctuations in the Davydov and Takeno models. Solid arrows, effect which a normalized fluctuation has at different phases of an oscillation; dotted arrows, effect which the multiplicative character of the noise has on a normalized fluctuation. Fluctuations in the Davydov model drive a local oscillator around the origin of phase space along an orbit of constant energy. Fluctuations in the Takeno model are impulsive, changing momentum without changing position, thus causing the system point jump between constant energy orbits. The multiplicative character of both types of fluctuation has the consequence that an oscillator experiences the same angular change during a unit fluctuation for any amplitude of the oscillator.

In the Takeno model noise also advances the phase of the oscillator in the same sense in all four quadrants of phase space; however, two characteristics of the noise prevent it from carrying the oscillator through complete cycles. First, since fluctuations in the Takeno model drive the momentum only, there is no fluctuation which carries the oscillator across constant-q surfaces; thus no sequence of fluctuations exists which can carry the oscillator through a complete cycle. Second, since fluctuations appear in the momentum equation multiplied by the position coordinate q, there exists one constant-q surface ($q=0$) in the neighborhood of which all fluctuations are vanishingly small. Since noise-driven excursions of phase in the Takeno model are *confined* relative to the *unbounded* excursions possible in the Davydov model, these geometrical considerations suggest that solitons of the Takeno model may enjoy a higher degree of stability against thermal fluctuations than do those of the Davydov model.

A related question is whether nonconservation of vibron number in the Takeno model should cause Takeno solitons to be less stable then Davydov solitons, since the loss of a conservation law opens up previously forbidden regions of phase space to the vibron system and affords more channels for decay. We note that the Takeno soliton is already an indefinite-number state and as such is a coherent structure in the full phase space. Second, fluctuations in the Takeno model cause changes in energy which stimulate a mechanical and/or thermodynamic response which generally opposes the fluctuation. Such restorative responses play no role in the Davydov model since the vibron system never leaves the constant-n surface.

On the other hand, in the absence of a number conservation law, it is possible that thermal fluctuations may decrease energy by changing the number of vibron quanta associated with a solitary-wave state as well as by changing wave-vector through scattering events. This observation suggests the existence of an optimal number of quanta and hence an optimal solitary wave may exist for each k. Such an optimal solitary wave should be exceptionally stable. To identify these optimal states, we minimize the total energy per quantum $\tilde{E}(k)/n$ with respect to the number of quanta n at fixed k

$$\left.\frac{\partial \tilde{E}(k)/n}{\partial n}\right|_k = 0 \ . \tag{8.6}$$

The solution (for $v_a \to \infty$) is found by inserting into (4.14) the particular value of the coupling constant given by

$$\sigma = \begin{cases} \dfrac{1}{2} - \dfrac{2k^2}{(k_0^*)^2} + \left[\dfrac{1}{4} + \dfrac{2k^2}{(k_0^*)^2}\right]^{1/2}, & 0 < k < k_0^* \quad (8.7a) \\ 0, \quad k > k_0^* \ . & (8.7b) \end{cases}$$

(See Fig. 7.)

We have thus identified the unique solitary-wave state for each wave vector k which has the lowest total energy consistent with that k. We note that the minimum energy envelope does not coincide with any "critical" energy

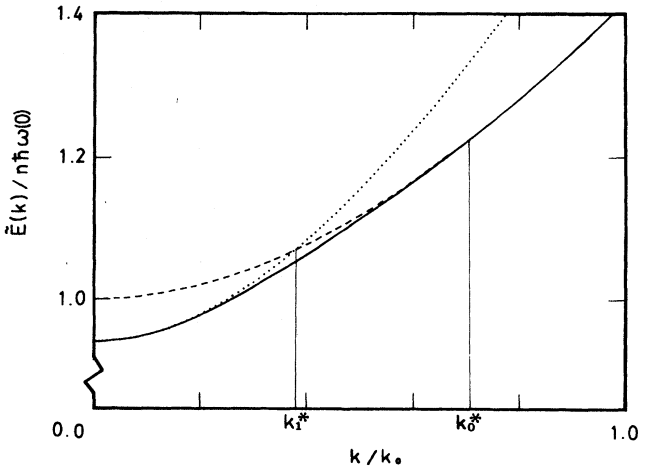

FIG. 7. Minimum energy envelope and related quantities. Solid line (——), minimum energy envelope; dashed line (— — —), linear energy; dotted line (· · · ·), critical energy. Note that the energy scale is broken; $[\hbar\omega(0)-\tilde{E}_c(0)]/\hbar\omega(0)\approx 5\%$.

(4.16c) except at $k=0$. The minimal solutions also distinguish themselves from other solitary-wave families in the k dependence of their widths (κ^{-1}). Every fixed-σ (e.g., fixed-n) family of solitary waves found in previous sections narrows monotonically with increasing k, in a manner consistent with the Lorentz invariance of the nonlinear Klein-Gordon equation. Quite a different behavior is found for the minimal solutions, whose width *increases* monotonically from a *minimum* width at $k=0$ to an *infinite* width at k_0^* and beyond.

On the basis of these findings, a qualitative description of thermalization can be given. A general epithermal state can be expected to relax quickly to a distribution along the minimum-energy envelope, resolving the initial distribution into short-wavelength $k > k_0^*$ plane waves and long wavelength $k < k_0^*$ solitary waves. The plane waves can be expected to relax along the linear dispersion curve toward k_0^* through number-conserving $k \to k'$ scattering, since number-nonconserving events are not energetically favored. Upon reaching k_0^*, number-nonconserving fluctuations play an increasingly important role since increases in the mean number of vibron quanta associated with the state become energetically favored. Below k_0^*, movement toward lower energies along the minimum energy envelope is accompanied by a decrease in the width of the relaxing state.

We thus arrive at the qualitative conclusion that *global energy minimization favors energy localization.*

IX. CONCLUSION

In this paper we have presented exact and approximate results which follow from our analysis of the Takeno Hamiltonian. We have obtained explicit solutions for the vibron coordinates in the form of solitary waves, and we have used these solutions to compute their energies and dispersion relations, as well as derivative quantities such as binding energies and effective masses. These results

are given in terms of material parameters, allowing quantitative description of the dynamics of vibrational energy transport. We have obtained particular solutions; however, by extracting general features such as nonlinear dispersion relations, one can form inferences concerning dynamical behavior not strictly subsumed by our solitary-wave states.

One general property of nonlinear waves which is exemplified in these results is the Benjamin-Feir instability governing the decay of a general state into solitary waves. We find that, consistent with Benjamin and Feir, a characteristic wave vector k_0^* separates regions of k space in which linear waves or solitary waves dominate dynamics. We have reached this conclusion, not by performing a formal stability analysis, but by examining the detail of the dependence of the total system energy on the wave vector k.

The Benjamin-Feir instability depends on the softening of the effective on-site vibron potential with increasing amplitude. The quadratic Takeno Hamiltonian includes this effect in the simplest way, at the cost of introducing an instability at finite amplitude. Attainment of the critical amplitude coincides with the attainment of the maximum binding energy and maximum redshift. These are given in this model as fixed fractions of the corresponding linear quantities. These fractions are independent of all other parameter values, and thus are good quantities with which to characterize the model.

In the weak-coupling limit, agreement with certain results of Davydov can be established. Binding energies and effective masses are found to agree in this limit, provided the vibron energy bandwidth is sufficiently wide relative to that of acoustic phonons; for narrow-band systems the two models yield different results even in weak coupling.

Our major conclusions are obtained in the continuum limit; however, we have investigated the influence of discreteness to leading order and have found that the principal effect of discreteness is to enhance binding energies, at least near the zone center.

By examining the dependence of the energy on the mean number of vibron quanta n as well as on the wave vector k, we have been able to infer certain characteristics of the mechanisms controling the decay of an excited state toward thermal equilibrium. First, we have shown that there exists a unique family of solitary waves which should be highly stable and should dominate dynamics. The existence of these states can be inferred from the fact that the solitary-wave energy band possesses a minimum-energy envelope. The existence of the minimum-energy envelope depends only on the qualitative requirement that the effective local potential softens with increasing amplitude; the shape of the envelope is characterized by three quantities: (1) the linear dispersion relation, (2) the Benjamin-Feir wave vector (k_0^*), and (3) the critical energy or amplitude ($\tilde{E}_c$ or q_c) at which the softening of the effective local potential ceases. Second, we have shown that thermal fluctuations in the Takeno model do not conserve vibron number, and hence allow transitions between fixed-n solitary-wave families. This opens up channels for decay which are forbidden to conserved quanta, and at first blush would appear to destabilize solitary wave states. Indeed, it would appear that over most of **k** space the greatest energy gain is to be had by changing vibron number and hence decaying out of a particular solitary-wave family labeled by n. However, all such decays bring the state of the system closer to the unique family of solitary waves which comprise the minimum-energy envelope.

These findings contrast with well-known characteristics of the Davydov model in which thermal fluctuations are number conserving. The principal effect which number-conserving fluctuations have on a state is to decrease energy through phase randomization—damping—one manifestation of which is a decreasing group velocity. In the Davydov model, decreasing group velocity is accompanied by a *broadening* of the solitary-wave state toward the characteristic width of the $k=0$ state set by the coupling strength and the (fixed) number of quanta. The number-nonconserving fluctuations in the Takeno model also cause damping, which would be manifested on the minimum-energy envelope by movement toward $k=0$. Unlike any fixed-n family of solitary waves in either the Takeno or Davydov models, movement toward $k=0$ along the minimum-energy envelope is accompanied by a *narrowing* of the solitary wave towards its minimum value at $k=0$.

We conclude that global energy minimization favors energy localization.

ACKNOWLEDGMENTS

This work was supported in part by U.S. Defense Advanced Research Projects Agency (DARPA) Contract No. DAAG-29-K-0246, and in part by National Science Foundation Grant No. DMR-86-19650-A1. The authors wish to thank Professor S. Takeno of Kyoto Technical University for numerous useful discussions and for making results of his research available prior to publication. The authors also wish to extend their thanks to Albert Migliori of Los Alamos National Laboratory for useful discussions and for making his results available to us prior to publication.

APPENDIX A

Substituting the trial solution (4.4) into (4.8) and equating coefficients of $\sin[kx-\tilde{\omega}(k)t]$ and $\cos[kx-\tilde{\omega}(k)t]$, respectively, we obtain two independent requirements for (4.8) to be satisfied; the first is (4.10a), and the second is the envelope equation

$$\frac{\partial^2\phi}{\partial x^2}=A\phi-B\phi^3 , \tag{A1}$$

where we have defined the coefficients A and B by

$$A=\gamma_f^2[\omega^2(k)-\tilde{\omega}^2(k)]/v_f^2 , \tag{A2}$$

$$B=\gamma_f^2\frac{G(v)}{\mu v_f^2} . \tag{A3}$$

Solving Eq. (A1) subject to the boundary conditions (7.7) yields the envelope function $\phi(x)$ having the familiar form

$$\phi(x)=\sqrt{2A/B}\,\mathrm{sech}(\sqrt{A}\,x)\ . \tag{A4}$$

which identifies

$$\kappa=\sqrt{A}\ , \tag{A5}$$

and

$$\phi_0=\sqrt{2A/B}\ . \tag{A6}$$

The carrier wave frequency $\tilde{\omega}(k)$ is implicitly contained in A and cannot be determined unless the amplitude of the soliton envelope is known. This amplitude should be fixed by the area under the soliton envelope. One quantity which is closely related to the area is the number of the vibron quanta. In the linear system, i.e., for free vibrons, the virial theorem provides that the normal modes have the property

$$\int_{-\infty}^{\infty} dx\ \tfrac{1}{2}\mu\omega^2(k)\overline{q^2(x,t)}=\tfrac{1}{2}n\hbar\omega(k)\ , \tag{A7a}$$

$$\int_{-\infty}^{\infty} dx\,\frac{\overline{p^2(x,t)}}{2\mu}=\tfrac{1}{2}n\hbar\omega(k)\ . \tag{A7b}$$

In the nonlinear system, our quantization hypothesis (4.12b) has the consequence that the virial integrals (A7) are replaced by

$$\int_{-\infty}^{\infty} dx\ \tfrac{1}{2}\mu\tilde{\omega}^2(k)\overline{q^2(x,t)}\approx\int_{-\infty}^{\infty} dx\ \tfrac{1}{2}\mu\tilde{\omega}^2(k)[\tfrac{1}{2}\phi^2(x,t)]$$
$$=\tfrac{1}{2}n\hbar\tilde{\omega}(k)\ , \tag{A8a}$$

$$\int_{-\infty}^{\infty} dx\,\frac{\overline{p^2(x,t)}}{2\mu}\approx\int_{-\infty}^{\infty} dx\,\frac{1}{2\mu}\left[\tfrac{1}{2}\tilde{\omega}^2(k)\phi^2(x,t)+\tfrac{1}{2}v^2\left[\frac{\partial\phi(x,t)}{\partial x}\right]^2\right]$$
$$=\tfrac{1}{2}n\hbar\tilde{\omega}(k)+\frac{n\hbar\kappa^2v^2}{6\tilde{\omega}(k)}\ , \tag{A8b}$$

in which we have implemented the RWA. The quantum number n so defined coincides with the number of the free-vibron quanta in the linear limit [defined as the expectation value of the operator $\hat{n}=\sum_n a_n^\dagger a_n$; cf. (1.6)]. The "anharmonic part" of (A8b), which is explicitly proportional to v^2, has a complex but interesting structure. If we retain only the lowest order in each of σ and v, and further consider only narrow bands ($v_f\ll v_a$), then this term can be put into the form

$$\frac{n\hbar\kappa^2v^2}{6\tilde{\omega}(k)}\approx\tfrac{1}{4}(nm^T-m^T_{\mathrm{sol}})v^2\ , \tag{A9}$$

which appears to be half of the kinetic energy associated with the "missing mass." The "other" half can be found in the kinetic energy of the lattice deformation (see Table I).

To find the phonon variables we apply the RWA and determine the lattice coordinates and momenta from the condition that the last two terms in (4.7) cancel,[18] which leads to

$$\overline{Q(x,t)}=-\gamma_a^2\frac{2g}{\zeta}\int_{-\infty}^{x} dy\ \overline{q^2(y)}$$
$$=-\gamma_a^2\frac{n\hbar g}{\zeta\mu\tilde{\omega}(k)}\tanh[\kappa(x-vt)] \tag{A10}$$

which is equivalent to (4.9b).

The total energy of the system is given by the expectation value of the Hamiltonian, as in (4.11). Although the total energy is a conserved quantity, we have introduced the rotating-wave approximation and thus need to average the Hamiltonian over a few vibron oscillations for consistency. Thus, in the continuum limit, we have

$$\tilde{E}=\int_{-\infty}^{\infty} dx\left[\tfrac{1}{2}\mu\omega^2(0)\overline{q^2(x,t)}+\frac{\mu}{2}\overline{\dot{q}^2(x,t)}+\frac{\mu v_f^2}{2}\overline{[\nabla_x q(x,t)]^2}\right]$$
$$+\int_{-\infty}^{\infty} dx\left[\frac{\zeta}{2}\overline{\nabla_x Q(x,t)^2}+\frac{1}{2\eta}\overline{P^2(x,t)}+2g\overline{\nabla_x Q(x,t)q^2(x,t)}\right]\ . \tag{A11}$$

Using the solution of $q(x,t)$ and $Q(x,t)$, each of the above terms can be integrated as given in Table I. The summation of all terms in (A11) yields

$$\tilde{E}=\frac{1}{2}\left[\frac{\omega^2(0)}{\tilde{\omega}^2(k)}+1+\frac{v^2}{v_f^2}\right]n\hbar\tilde{\omega}(k)$$
$$+\frac{1}{3}\left[\frac{1}{2}\left[1+\frac{v^2}{v_f^2}\right]+\left[1+\frac{v^2}{v_a^2}\right]\frac{\gamma_a^2}{\gamma_f^2}-\frac{2}{\gamma_f^2}\right]\times\left[\frac{\kappa v_f}{\tilde{\omega}(k)}\right]^2 n\hbar\tilde{\omega}(k)\ . \tag{A12}$$

Using (A2) and (A5), κ can be eliminated

$$\tilde{E}=\left[\frac{2}{3}\frac{\gamma_f^2-\gamma_a^2+1}{\gamma_f^2}\left[\frac{\tilde{\omega}(k)}{\omega(0)}-\frac{\gamma_f^2\omega(0)}{\tilde{\omega}(k)}\right]+\frac{\gamma_f^2\omega(0)}{\tilde{\omega}(k)}\right]n\hbar\omega(0)\ , \tag{A13}$$

and using $\tilde{\omega}(k)$ from (4.14), we can then obtain (4.15f) or (4.19).

In the linear limit, $\tilde{\omega}(k)$ goes to $\omega(k)$, and we see from (A13) that the energy of the system goes to the linear energy $n\hbar\omega(k)$, verifying that the n defined in (4.12b) does give rise to the correct vibron number in the linear limit.

In the case where v and σ both are small, Taylor expansion of (A13) yields

$$\tilde{E}\approx\left[1-\frac{\sigma^2}{24}+\frac{1}{2}\frac{v^2}{v_f^2}+\frac{1}{12}\frac{v^2}{v_a^2}\left[1-\frac{1}{4}\frac{v_a^2}{v_f^2}\right]\sigma^2\right]n\hbar\omega(0) \tag{A14}$$

from which (4.22)–(4.25) can be obtained.

TABLE I. Integration results for computing energies in the solitary-wave state; continuum limit.

Contribution to $\tilde{E}$	Integration result
$\int_{-\infty}^{\infty} dx\, \frac{1}{2}\mu\omega^2(0)\overline{q^2(x,t)}$	$\frac{1}{2}\left[\frac{\omega(0)}{\tilde{\omega}(k)}\right]^2 n\hbar\tilde{\omega}(k)$
$\int_{-\infty}^{\infty} dx \frac{\mu}{2}\overline{\dot{q}^2(x,t)}$	$\frac{1}{2}\left[1+\frac{1}{3}\frac{v^2}{v_f^2}\left[\frac{\kappa v_f}{\tilde{\omega}(k)}\right]^2\right] n\hbar\tilde{\omega}(k)$
$\int_{-\infty}^{\infty} dx \frac{\mu v_f^2}{2}\overline{[\nabla_x q(x,t)]^2}$	$\frac{1}{2}\left[\frac{v^2}{v_f^2}+\frac{1}{3}\left[\frac{\kappa v_f}{\tilde{\omega}(k)}\right]^2\right] n\hbar\tilde{\omega}(k)$
$\int_{-\infty}^{\infty} dx \frac{\overline{\zeta[\nabla_x Q(x,t)]^2}}{2}$	$\frac{1}{3}\frac{\gamma_a^2}{\gamma_f^2}\left[\frac{\kappa v_f}{\tilde{\omega}(k)}\right]^2 n\hbar\tilde{\omega}(k)$
$\int_{-\infty}^{\infty} dx \frac{\overline{P^2(x,t)}}{2\eta}$	$\frac{1}{3}\frac{\gamma_a^2}{\gamma_f^2}\frac{v^2}{v_a^2}\left[\frac{\kappa v_f}{\tilde{\omega}(k)}\right]^2 n\hbar\tilde{\omega}(k)$
$\int_{-\infty}^{\infty} dx\, 2g\overline{\nabla_x Q(x,t) q^2(x,t)}$	$-\frac{2}{3\gamma_f^2}\left[\frac{\kappa v_f}{\tilde{\omega}(k)}\right]^2 n\hbar\tilde{\omega}(k)$

APPENDIX B

The solution for the case with discreteness corrections can be found by substituting the trial function (4.4) into (6.2). We obtain two independent conditions which must hold in order for (6.2) to be satisfied; the first is (4.10a), and the second is the envelope equation which now is modified by a discreteness correction term

$$\frac{\partial^2\phi}{\partial x^2} = A\phi - B\phi^3 + C\phi\frac{\partial^2\phi}{\partial x^2} . \tag{B1}$$

A and B are defined as in (A2) and (A3), and the new coefficient C is defined by

$$C \equiv \frac{l^2}{4}B = \frac{l^2}{4}\gamma_f^2\frac{G(v)}{\mu v_f^2} . \tag{B2}$$

Equation (B1) can be integrated once to obtain the "energy" relation

$$\frac{E}{1+2C\phi^2} = \frac{1}{2}\left[\frac{\partial\phi}{\partial x}\right]^2 + \frac{1}{2}\left[\frac{-A\phi^2+\frac{1}{2}B\phi^4}{1+2C\phi^2}\right] , \tag{B3}$$

where E is an integration constant. The boundary conditions (7.7) for localized solutions can be satisfied by setting $E=0$ (see also Ref. 18). The peak amplitude is given by the zero of the "potential" in the same manner as in the continuum case

$$\phi_0 = \left[\frac{2A}{B}\right]^{1/2} = \left[\frac{2\mu[\omega^2(k)-\tilde{\omega}^2(k)]}{G(v)}\right]^{1/2} . \tag{B4}$$

Thus, the envelope function is given by inverting the integral

$$x = \frac{1}{\sqrt{D}}\int_1^{\phi/\phi_0} du \frac{1}{u}\left[\frac{1+Du^2}{1-u^2}\right]^{1/2} . \tag{B5}$$

The shape of the envelope is controlled by the parameter D, which is a measure of the importance of the discreteness of the medium. D is given by

$$D = 2C\phi_0^2 . \tag{B6}$$

The relationship of D to κ cannot be completely determined without inverting (B5); however, the limiting behaviors of the envelope function are easily seen to be given by

$$\phi = \begin{cases} \phi_0 \operatorname{sech}(\kappa x), & D \ll 1 \quad \text{(B7a)} \\ \phi_0 \cos\left[\frac{\pi}{4}(\kappa x)\right], & D \gg 1 , \quad \text{(B7b)} \end{cases}$$

and allows us to show that

$$\kappa = \begin{cases} \sqrt{D}\, l^{-1}, & D \ll 1 \quad \text{(B8a)} \\ \frac{4}{\pi l}, & D \gg 1 . \quad \text{(B8b)} \end{cases}$$

and

$$D = \begin{cases} \frac{1}{4}\frac{\sigma^2}{\tilde{\omega}^2(k)}\left[\frac{l\omega^2(0)}{v_f}\right]^2, & D \ll 1 \quad \text{(B9a)} \\ \frac{2}{\pi}\frac{\sigma}{\tilde{\omega}(k)}\left[\frac{l\omega^2(0)}{v_f}\right], & D \gg 1 . \quad \text{(B9b)} \end{cases}$$

The introduction of the scale factor $\pi/4$ into (B7) and (B8) is somewhat arbitrary, but this choice of scaling results in a definition of κ consistent with the quantization hypothesis (4.12b), which results in replacing the virial

TABLE II. Integration results for computing energies in the solitary-wave state; leading correction to the continuum limit.

Contribution to $\tilde{E}$	Integration result
$\int_{-\infty}^{\infty} dx \frac{\mu}{2}\omega^2(0)\overline{q^2(x,t)}$	$\frac{1}{2}\left[\frac{\omega(0)}{\tilde{\omega}(k)}\right]^2 n\hbar\tilde{\omega}(k)$
$\int_{-\infty}^{\infty} dx \frac{\mu}{2}\overline{\dot{q}^2(x,t)}$	$\frac{1}{2}\left[1+\left[\frac{v_f}{l\tilde{\omega}(k)}\right]^2\frac{v^2}{v_f^2}\right]n\hbar\tilde{\omega}(k)$
$\int_{-\infty}^{\infty} dx \frac{\mu v_f^2}{2}\overline{[\nabla_x q(x,t)]^2}$	$\frac{1}{2}\left[\frac{v^2}{v_f^2}+\left[\frac{v_f}{l\tilde{\omega}(k)}\right]^2\right]n\hbar\tilde{\omega}(k)$
$\int_{-\infty}^{\infty} dx \frac{\zeta\overline{[\nabla_x Q(x,t)]^2}}{2}$	$\frac{3\gamma_a^2}{4}\frac{n^2\hbar^2 G(v)}{\pi l\mu^2\tilde{\omega}^2(k)}$
$\int_{-\infty}^{\infty} dx \frac{\overline{P^2(x,t)}}{2\eta}$	$\frac{3\gamma_a^2}{4}\frac{v^2}{v_a^2}\frac{n^2\hbar^2 G(v)}{\pi l\mu^2\tilde{\omega}^2(k)}$
$\int_{-\infty}^{\infty} dx\, 2g\overline{\nabla_x Q(x,t)q^2(x,t)}$	$-\frac{3}{2}\frac{n^2\hbar^2 G(v)}{\pi l\mu^2\tilde{\omega}^2(k)}$

integrals (A7) with

$$\int_{-\infty}^{\infty} dx\, \tfrac{1}{2}\mu\tilde{\omega}^2(k)\overline{q^2(x,t)} \approx \int_{-\infty}^{\infty} dx\, \tfrac{1}{2}\mu\tilde{\omega}^2(k)[\tfrac{1}{2}\phi^2(x,t)] = \tfrac{1}{2}n\hbar\tilde{\omega}(k)\ , \tag{B10a}$$

$$\int_{-\infty}^{\infty} dx \frac{\overline{p^2(x,t)}}{2\mu} \approx \int_{-\infty}^{\infty} dx \frac{1}{2\mu}\left[\frac{1}{2}\tilde{\omega}^2(k)\phi^2(x,t) + \frac{1}{2}v^2\left[\frac{\partial\phi(x,t)}{\partial x}\right]^2\right] = \tfrac{1}{2}n\hbar\tilde{\omega}(k)\left[1+\left[\frac{\pi}{4}\right]^2\frac{\kappa^2 v^2}{[\tilde{\omega}(k)]^2}\right]. \tag{B10b}$$

The various contributions to the total energy in the high discreteness case are given in Table II. Combining all these contributions, the total energy is given by

$$\tilde{E}_{\rm tot} = \frac{1}{2}\left[\left[\frac{\omega(0)}{\tilde{\omega}(k)}\right]^2 + \left[1+\frac{v^2}{v_f^2}\right]\left[1+\frac{v_a^2}{l^2\tilde{\omega}^2(k)}\right]\right]n\hbar\tilde{\omega}(k) + \left[\frac{3}{4}\frac{v_a^2+v^2}{v_a^2-v^2}-\frac{3}{2}\right]\frac{n^2\hbar^2 G(v)}{\pi l\mu^2\tilde{\omega}^2(k)}\ . \tag{B11}$$

With the help of (6.5), $G(v)$ can be eliminated, yielding

$$\tilde{E} = \frac{1}{8\gamma_f r}\left[(8\gamma_f^2-6\gamma_a^2+5)r^2+6\gamma_a^2-5 + \left[1+\frac{v^2}{v_f^2}\right]\frac{8}{3D_{\max}}\right]n\hbar\omega(0)\ , \tag{B12}$$

wherein $r=\tilde{\omega}(k)/\gamma_f\omega(0)$. The zero-velocity part of (B12) is given in (6.11).

[1] A. S. Davydov and N. I. Kislukha, Phys. Status Solidi **59**, 465 (1973); Zh. Eksp. Teor. Fiz. **71**, 1090 (1976) [Sov. Phys.—JETP **44**, 571 (1976)].

[2] L. D. Landau, Phys. Z. Sowjetunion **3**, 664 (1933).

[3] S. I. Pekar, J. Phys. USSR **10**, 341 (1946); *Untersuchungen Uber die Elektronentheorie der Kristalle* (Akademie-Verlag, Berlin, 1954).

[4] L. D. Landau and S. I. Pekar, Zh. Eksp. Teor. Fiz. **18**, 419 (1948).

[5] H. Fröhlich, H. Pelzer, and S. Zieman, Philos. Mag. **41**, 221 (1950); Proc. R. Soc. London, Ser. A **215**, 291 (1952); Adv. Phys. **3**, 325 (1954).

[6] E. I. Rashba, Opt. Spektrosk. **2** (1957); **3**, 568 (1957).

[7] T. Holstein, Ann. Phys. (N.Y.) **8**, 325 (1959).

[8] A. S. Davydov, Phys. Status Solidi **36**, 211 (1969).

[9] A. S. Davydov, Phys. Scr. **20**, 387 (1979); Usp. Fiz. Nauk **138**, 603 (1982) [Sov. Phys.—Usp. **25**, 898 (1982)].

[10] A. S. Davydov, Zh. Eksp. Teor. Fiz. **51**, 789 (1980) [Sov. Phys.—JETP **78**, 397 (1980)].

[11] A. C. Scott, Phys. Rev. A **26**, 587 (1982); **27**, 2767 (1982).

[12] G. Careri, U. Buontempo, F. Carta, E. Gratton, and A. C. Scott, Phys. Rev. Lett. **51**, 304 (1983).

[13] G. Careri, U. Buontempto, F. Galluzi, A. C. Scott, E. Gratton, and E. Shyamsunder, Phys. Rev. B **30**, 4689 (1984).

[14] J. C. Eilbeck, P. S. Lomdahl, and A. C. Scott, Phys. Rev. B **30**, 4703 (1984).

[15] P. S. Lomdahl and W. C. Kerr, Phys. Rev. Lett. **55**, 1235 (1985).

[16] Albert F. Lawrence, James C. McDaniel, David B. Chang, Brian M. Pierce, and Robert R. Birge, Phys. Rev. A **33**, 1188 (1986).

[17] L. Cruzeiro, J. Halding, P. L. Christiansen, O. Skovgaard, and A. C. Scott, Phys. Rev. A **37**, 880 (1988).

[18] Xidi Wang, David W. Brown, Katja Lindenberg, and Bruce J. West, Phys. Rev. A **37**, 3557 (1988).

[19] A. C. Scott, E. Gratton, E. Shyamsunder, and G. Careri, Phys. Rev. B **32**, 5551 (1985).

[20] A. C. Scott, Philos. Trans. R. Soc. London, Ser. A **315**, 423

(1985).
[21]B. J. West and K. Lindenberg, J. Chem. Phys. **83**, 4118 (1985).
[22]David W. Brown, Katja Lindenberg, and Bruce J. West, J. Chem. Phys. **84**, 1574 (1986).
[23]David W. Brown, Katja Lindenberg, and Bruce J. West, Phys. Rev. A **33**, 4110 (1986).
[24]David W. Brown, Katja Lindenberg, Bruce J. West, Jeffry A. China, and Robert Silbey, J. Chem. Phys. **87**, 6700 (1987).
[25]D. M. Alexander, Phys. Rev. Lett. **54**, 138 (1985); D. M. Alexander and J. A. Krumhansl, Phys. Rev. B **33**, 7172 (1986).
[26]David W. Brown, Katja Lindenberg, and Bruce J. West, Phys. Rev. A **33**, 4014 (1986).
[27]W. C. Kerr and P. S. Lomdahl, Phys. Rev. B **35**, 3629 (1987).
[28]D. W. Brown, K. Lindenberg, and B. J. West, in *Nonlinearity in Condensed Matter,* Vol. 69 of *Springer Series in Solid-State Sciences,* edited by A. R. Bishop, D. K. Campbell, P. Kumar, and S. E. Trullinger (Springer-Verlag, Berlin, 1987).
[29]David W. Brown, Phys. Rev. A **37**, 5010 (1988).
[30]D. W. Brown, K. Lindenberg, and B. J. West, Phys. Rev. Lett. **57**, 2341 (1986); **57**, 3124 (1986); Phys. Rev. B **35**, 6169 (1987).
[31]G. Venzl and S. F. Fischer, J. Chem. Phys. **81**, 6090 (1984); Phys. Rev. B **32**, 6437 (1985).
[32]Q. Zhang, V. Romero-Rochin, and R. Silbey, Phys. Rev. A **38**, 6409 (1988).
[33]M. J. Skrinjar, D. V. Kapor, and S. D. Stojanovic, Phys. Rev. A **38**, 6402 (1988).
[34]S. Takeno, Prog. Theor. Phys. **71**, 395 (1984).
[35]S. Takeno, Prog. Theor. Phys. **73**, 853 (1985).
[36]S. Takeno, Prog. Theor. Phys. **75**, 1 (1985).
[37]P. S. Lomdahl and W. C. Kerr, in *Physics of Many Particle Systems,* edited by A. S. Davydov (Naukova Dumka, Kiev, 1988).
[38]N. A. Nevskaya and Yu N. Chirgadze, Biopolymers **15**, 637 (1976).
[39]A. Migliori, P. M. Maxton, A. M. Clogston, E. Zirngiebl, and M. Lowe, Phys. Rev. B **38**, 13 464 (1988).
[40]R. J. Glauber, Phys. Rev. **131**, 2766 (1963).
[41]William H. Louiselle, *Quantum Statistical Properties of Radiation* (Wiley, New York, 1973).
[42]A. S. Davydov, *Solitons in Molecular Systems* (Reidel, Boston, 1985).
[43]T. B. Benjamin and J. F. Feir, J. Fluid Mech. **27**, 417 (1967).
[44]A. C. Newell, *Solitons in Mathematics and Physics* (Society for Industrial and Applied Mathematics, Philadelphia, 1985).
[45]G. B. Whithman, *Linear and Nonlinear Waves* (Wiley, New York, 1974).
[46]See, e.g., O. Madelung, *Introduction to Solid State Theory,* Vol. 2 of *Springer Series in Solid-State Sciences,* edited by M. Cardona, P. Fulde, and H.-J. Queisser (Springer-Verlag, Berlin, 1978).
[47]S. Takeno, K. Kisoda, J. Phys. Soc. Jpn. **57**, 675 (1988).
[48]See, e.g., R. Kubo, in *Stochastic Processes in Chemical Physics,* Vol. XV of *Advances in Chemical Physics,* edited by K. E. Shuler (Wiley-Interscience, New York, 1969), and references therein.